Supplementary Information for
Late Mid-Pleistocene hominin fire control inferred from sooty speleothem analysis

Ségolène Vandevelde*, Edwige Pons-Branchu, Damien Deldicque, Abdou Niane, Cyrielle Mathias, Dany Savard, Yves Perrette, Bruno Desachy, Ludovic Slimak, Kevin Bouchard

DOI: 10.1007/s10816-025-09709-5

Main text available at: https://doi.org/10.1007/s10816-025-09709-5.

This PDF file includes:

Supplementary Note 1 – Early traces of fire in western Europe

Table S1. Early traces of fire in archaeological sites in western Europe. Data are visually presented in Figure 1 (Main text). Yes*: but not in archaeological level where fire traces are documented.

	Site	Chronology	Human remains	Remains	References
1	Gruta da Aroeira, X	MIS 11	yes	Byproducts of combustion	(Montserrat Sanz et al. 2018, 2020)
2	Valdocarros II, levels I and II	~245 ka, MIS 8/7	no	Hearths, lipid biomarkers	(Stancampiano et al., 2023)
3	La Solana del Zamborino	750 ky or 408–300 ky	no	Built hearth?	(Bister 2005)
4	Cueva Negra del Estrecho del Río Quípar	800 ky	no	Burnt bones, charcoal, combustion structures	(Walker et al. 2016a)
5	Bolomor, XIII, XI, IV, II	MIS 7 and 6 and 5e	yes	Combustion structures (3 in layer IV), ashes, coals, heated lithics, 2 built hearths (layer XIII)	(Blasco 2006; Fernándes-Peris 2007a; Blasco and Peris 2009; Fernández Peris et al. 2012; Arsuaga et al. 2012; Sañudo et al. 2016)
6	Cansaladeta, layers D, L, C and A	MIS 11 (372 ± 34 ka - TL layer D) / MIS 14/15? (~600 ka - biochronology layer L)	no	Little evidence of fire: Heat damage recorded on bones and lithic remains (TL dating on burnt chert in layer D) and micro-charcoal concentrations in layers L, C and A. But no combustion areas or combustion structure, neither macro-charcoals are documented	(Ollé et al. 2016)
7	Menez-Dregan, 9, 7, 6', 5e, 5d, 5c, 4c	MIS 12/11 and MIS 9 and MIS 7	no	Combustion structures (scattered charcoal and heated lithics for 4c-5, MIS7)	(Mercier et al. 2004; Monnier et al. 1994a, 2001; Ravon et al. 2022)
8	La Cotte de Saint Brelade, C-D	MIS 7/6 (238 ± 35 ky TL)	no	Some scattered charcoal, heated lithics, and burnt bones	(Callow and Cornford 1986; Hérisson et al. 2013)
9	Gouberville, two occupation levels	MIS 6 (187 ± 26 ky; 128 ± 20 ky TL)	no	Very little evidence of fire: a few heated flints (on which TL dating has been applied)	(Kolen 2000)
10	La Roche Gélétan	MIS 6 (149 ± 11 ky TL)	no	Built hearth	(Cliquet et al. 2003; Cliquet and Lautridou 2009; Hérisson et al. 2013)
11	Port Pignot	MIS 7/6	no	Built hearth	(Cliquet et al. 2003; Cliquet and Lautridou 2009; Hérisson et al. 2013)
12	Grossoeuvre, two occupation levels in a doline	MIS 7 (end) - MIS 5 (220 ± 12 ky; 130 ± 8 ky TL)	no	Very little evidence of fire: a few heated flints (on which TL dating has been applied)	(Cliquet et al. 2003)
13	Pontnewydd	MIS 7 (200±25 ka; 269 ± 37 ka - TL)	no	Very little evidence of fire: a few heated flints (on which TL dating has been applied)	(Aldhouse Green et al. 2012)
14	Beeches Pit, 3b, 5 and 6	MIS 11	no	Combustion structures	(Gowlett et al. 2005; Gowlett 2006; Preece et al. 2006a)
15	Therdonne - N3	MIS 6 (178 ± 11 ky)	no	Numerous burnt flints and rare burnt faunal remains + several areas rich in organic residues and wood microcharcoal (remains of combustion structures?)	(Locht et al. 2010; Hérisson et al. 2013)
16	Revelles, Les Terres-Sellier	MIS 9 (291.6 ± 28 ka, 263.6 ± 26.2 ka – TL)	no	Very little evidence of fire: a few heated flints (on which TL dating has been applied)	(Coutard et al. 2019; Lamotte et al. 2019)
17	Biache-Saint-Vaast - E, IIa, IIbase, D1	MIS 7 (IIa 175 ky -> MIS 6)	yes	Evidence of combustion: burnt flint and faunal remains and sometimes charcoal	(Truffeau and Sommé 1988; Guipert et al. 2011; Hérisson et al. 2013)

	Site	Chronology	Human remains	Remains	References
18	Etricourt-Manancourt, level HUD	MIS 9 (274 ± 32 ka, 294 ± 25 ka, 288 ± 26 ka – TL)	no	Very little evidence of fire: a few heated flints (on which TL dating has been applied)	(Hérisson et al. 2016; Coutard et al. 2018)
19	La Grande Vallée	MIS 11-13 (possibly 10-15? Max: 350-600 ka)	no	Very little evidence of fire: a few heated flints (on which TL dating has been applied)	(Hérisson et al. 2012)
20	Abri Suard, level 51	MIS 6 (126 ± 15 ka – TL)	yes	Very little evidence of fire: a few heated flints (on which TL dating has been applied)	(Schvoerer et al. 1977; Coqueugnot et al. 1996; Couture-Veschambre et al. 2021)
21	Petit Bost layer 2	MIS 9–8	no	Very little evidence of fire: a few heated flints (on which TL dating has been applied)	(Bourguignon et al. 2008)
22	Combe Brune 2, V, VI, VIIb and X	MIS 7 (X, 195 ± 16 ka - TL) and MIS 6 (V, 183 ± 20 ka; VI, 185 ± 23 ka; VIIb, 187 ± 21 ka - TL)	no	Very little evidence of fire: a few heated flints (on which TL dating has been applied)	(Brenet et al. 2014)
23	Combe Brune 3	MIS 6 (156.4 ± 11.7 ky TL)	no	Very little evidence of fire: a few heated flints (on which TL dating has been applied)	(Brenet et al. 2006; 2014)
24	Barbas I, layers C'3base and C'4	MIS 7 (C'4, 239 ± 44 ka - TL) and MIS 6 (C'3base, 146 ± 29, 147± 28 TL)	no	Very little evidence of fire: a few heated flints (on which TL dating has been applied)	(Valladas et al. 1999; Boëda et al. 2000)
25	Cantalouette I, layer V	MIS 7 (222.9 ± 20.1 ka – TL)	no	Very little evidence of fire: a few heated flints (on which TL dating has been applied)	(Vieillevigne et al. 2008)
26	Cantalouette II, base	MIS 6 (165 ± 13 ka – TL)	no	Very little evidence of fire: a few heated flints (on which TL dating has been applied)	(Brenet et al. 2014)
27	Pech-de-l'Azé II (layer 7, levels b and c)	MIS 7/6 - 140–180 ky	no	Built hearth	(Bordes 1971; Jacobs et al. 2016; Stratus 1989)
28	Vaufrey, layers VIII and IV	MIS 7? (VIII) and MIS 6 (IV, 165 ± 13 ka - TL)	no	VIII. Localized charcoals and burnt bones (= remains of combustion structures?). No structured hearth. IV. very little evidence of fire: a few heated flints (on which TL dating has been applied)	(Rigaud 1988a; Rigaud and Geneste 1988)
29	Les Bosses	MIS 8? (ca. 300 ky)	no	Very little evidence of fire: a few heated flints (on which TL dating has been applied)	(Jarry et al. 2004)
30	Bruniquel	MIS 6	no	Combustion structure	(Jaubert et al. 2016)
31	Coupe-Gorge, levels 3Z, 3Y	MIS 7 or 6	yes	Old excavations: hearth reported from layer 3Z and 3Y, associated with heated bones and lithics, heated cobbles and charcoals	(Gaillard 1979, citing L. Méroc's work in the 1950's)
32	Caune de l'Arago	MIS 14 (ca. 560 ky)	yes*	Chars + heated minerals	(Deldicque et al. 2021)
33	Payre, G-F	MIS 8 and MIS 7	yes	Combustion structure, burnt elements, occasional use of bone as fuel	(Moncel et al. 2008; Daujeard and Moncel 2010)
34	Bau de l'Aubesier, H1	MIS 7-6 (169 ± 17 ky, 191 ± 15 ky TL)	yes	Combustion structure	(Lebel et al. 2001, 2007; Lebel and Trinkaus 2002)

	Site	Chronology	Human remains	Remains	References
35	Terra Amata	MIS 11 or MIS 11–9? (380 ± 80 ky – ESR), 239 ± 40 ky – TL)	no	Built hearth	(Villa 1983, 1991; Falguères et al. 1988b; Lumley et al. 2016)
36	Lazaret	MIS 6	yes	Combustion structure	(Kolen 2000; Lumley et al. 2004)
37	Maastricht-Belvédère (Unit 4)	MIS 7 (250 ± 22 ky)	no	Combustion structures (clusters of charcoal and heated flints)	(Roebroeks 1988; Stapert 2007; Hérisson et al. 2013)
38	Tönchesberg, level 2A	MIS 6	no	Very little evidence of fire: a few heated flints (on which TL dating has been applied)	(Schmidt et al. 2011)
39	Schöningen 13 II-4 + above Schöningen 12?	MIS 11–9 and more recent above Schöningen 12	no	Combustion structure(?) in which charred pieces of wood have been preserved (Schöningen 12) + charred wooden tools (Schöningen 13 II-4) + heated natural flint fragments do indicate fire (natural or anthropogenic)	(Burdukiewicz 2021; Schiegl and Thieme 2007a)
40	Bilzingsleben	MIS 11–9	yes	Burnt bones, burnt lithics, and charcoal, magnetic susceptibility	(Mania 1991; Street et al. 2006)
41	Ehringsdorf	MIS 7	yes	Charcoal and charred/burnt bones	(Behm-Blancke 1960; Hérisson et al. 2013; Schafer and Jager 1984; Steiner 1975; Street et al. 2006)
42	Campitello Quarry	MIS 7 (end)	no	Use for tool shafting (birch bark tar on two flints)	(Mazza et al. 2006)
43	Poggetti Vecchi	MIS 7; 171 ky	no	Wooden tool making using fire	(Aranguren et al. 2018; Benvenuti et al. 2017)
44	Moravský Krumlov IV	MIS 6	no	Charcoal and charred/burnt bones	(Nerudová and Neruda, 2009)
45	Stránská skylá 1	MIS 17–16	no	Some burnt flints and bones	(Valoch 2003a; Burdukiewicz 2021)
46	Rozumice 3 (site C - layers 10, 7, 4)	MIS 8	no	Combustion structures (burnt bones in hearths)	(Foltyn et al. 2004, 2005)
47	Vérteszöllös	MIS 11/9?	yes	Old discovery of remains of fire, charcoal, charred fragments of animal bones (used as fuel?)	(Vertes and Dobosi 1990a; Soukup and Mechurová 2018a)
48	Medzhybizh	MIS 11	no	Heated and burnt bones, charcoals and heated sediments (only mentioned)	(Stepanchuk and Moigne 2016)

Supplementary Note 2 – Hominin designation

Seven human teeth were discovered at the Orgnac 3 site, all in the lower archaeological levels (AL 5a, 5b, 6). These include an upper right canine belonging to an adult, as well as six deciduous teeth (four molars and two incisors). Two of the molars were attributed to a 9-year-old child, whereas the incisors probably belonged to a 5-year-old child (Lumley 1976). The crowns of the teeth are much larger than those of *Homo sapiens* or classic Neanderthals. The second deciduous molar is rather elongated, with five cusps. There is significant mesio-distal elongation of the crown, a large, deep anterior fovea, and a large cervical bulge on the vestibular side. The lower second decidual molars are comparable to those found at the Arago Cave, at Tautavel in southern France (Arago I, V). M.-A. de Lumley (1982) linked the remains from Orgnac 3 to the Pre-Neanderthals. In the absence of recent detailed analysis, however, it remains difficult to position these dental remains precisely within a Middle Pleistocene evolutionary lineage. Further analysis of this material (ongoing work by Chevalier, personal communication) should provide new insights.

In Europe, the anthropological question for the late Acheulean and the early Middle Paleolithic remains uncertain. First, few fossils are associated with ancient deposits. Second, species attributions are sometimes difficult given the fragmentation of most remains, particularly for differentiating early Neanderthal and *Homo heidelbergensis*. The attribution names are thus heterogeneous in the literature; for example, human remains found at sites in Europe dated between MIS 9 and MIS 6 are generally divided among Neanderthals (ancient, classic), Pre-Neanderthals, *Homo heidelbergensis*, and *Homo erectus*. If we consider the available data, only a few human remains have been discovered at MIS 9 and MIS 8 aged sites in Europe, as only the sites of Orgnac 3 and Sedia Del Diavolo have a precise chronological framework (Mallegni 1986; Soriano and Villa 2017). From MIS 7 onward, the number of fossil remains increases considerably, with individuals attributed to Neanderthals and early Neanderthals, at sites such as Tourville-la-Riviere (Faivre et al. 2014), Pontnewydd (Compton and Stringer 2015; Green et al. 1981), Galeria Pesada (Trinkaus et al. 2003), and Casal de'Pazzi (Manzi et al. 1990; Pereira 2017). Some remains have even been attributed to archaic *Homo sapiens* at Apidima, Greece (Harvati et al. 2019).

Given the difficulty of assigning fossils in western Europe between MIS 9 and MIS 6, particularly with partial or isolated discoveries, we have chosen to use "Late Mid-Pleistocene hominins" to characterize the inhabitants of Orgnac 3 in this paper.

Supplementary Note 3 – Characterization of the black deposits

To identify the nature of the bluish-black laminae observed in Org3-fsp1, we performed EDX microprobe analyses (coupled with SEM) on Org-fsp1-s5a, a small section of the speleothem that we polished with diamond gel (1 µm) on cloth polishing disk for elemental analysis (Figures S1and S2).

Analyses were performed at the MAPS Platform, MSH Mondes, Nanterre, France, using a Zeiss EVO 10 conventional SEM with variable pressure coupled to an EDX detector to conduct spectral and mapping analysis.

The EDX analysis ruled out the hypothesis of metallic oxides being the cause of the black deposits, as the only measurable elements were Ca, C, O, and Si (other elements were below the detection limit) (Figure S3). It also revealed that the black deposits were well cemented within the carbonated fabric, as there was no significant difference in composition between the black laminae and the "clean carbonates" on elemental maps, which demonstrated a uniform distribution of elements (Figure S2). Similar findings were observed in other analyses of sooty speleothems, where thin layers of soot were found to stain the carbonates rather than thick layers of soot mixed with the carbonates (Bonneau et al. 2011; Gradziński et al. 2007; Martínez-Pillado et al. 2010, 2014). The absence of metallic oxides, the presence of particles appearing black and opaque in microscopy in reflected and transmitted lights (*cf.* Supplementary Note 4), and their cementation in carbonates, as observed in other studies, strongly indicate that the black films are composed of soot.

This identification was confirmed unequivocally through Raman microspectroscopy conducted on a black lamina from Org3-fsp1 at the Laboratoire de Géologie de l'ENS (École Normale supérieure, Paris, France). A Renishaw® inVia Raman microspectrometer equipped with a Cobolt 514 nm laser was used. Data were collected with a 5% laser intensity (2.5 mW) and a 30 s time exposure. All spectra obtained from the black films displayed two broad peaks around 1360–1365 and 1600–1610 cm^{-1} (as shown in Figures S4 and S5), which correspond to the D (defect) and G (graphite) bands of carbon (D. Deldicque et al. 2016). These signals are typical for solid products of the carbonization process. The comparable height and broad width of these bands indicate that the material consists of carbon layers with numerous defects, characteristic of soot. The third peak at 1085 cm^{-1} is specific to calcite.

All of these findings indicate that these black laminae are composed of carbonates stained with soot, which matches the deposits identified in previous studies (Bonneau et al. 2011; Gradziński et al. 2007; Vandevelde et al. 2017).

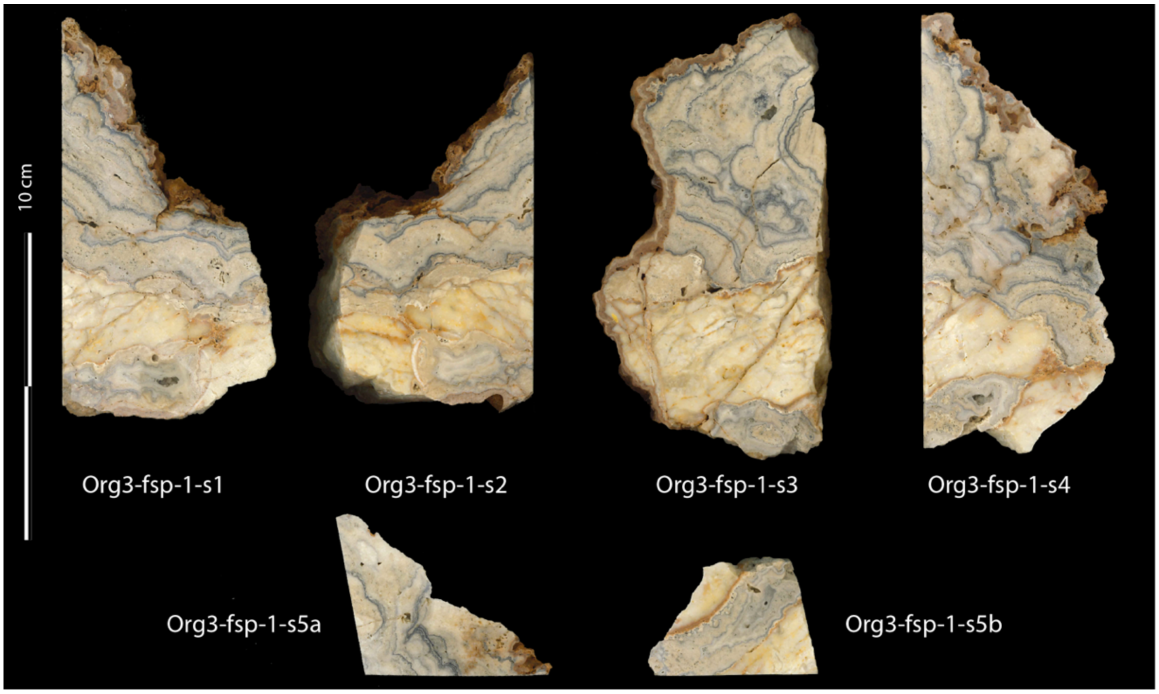

Figure S1. Sections of the Orgnac 3 fuliginous speleothem (Org3-fsp1). Note the budding coralloid-like structure of the speleothem. Sections 1 and 2 were cut along the growth axis, perpendicular to calcite laminae to facilitate a chronological study of the sooty speleothem formation process.

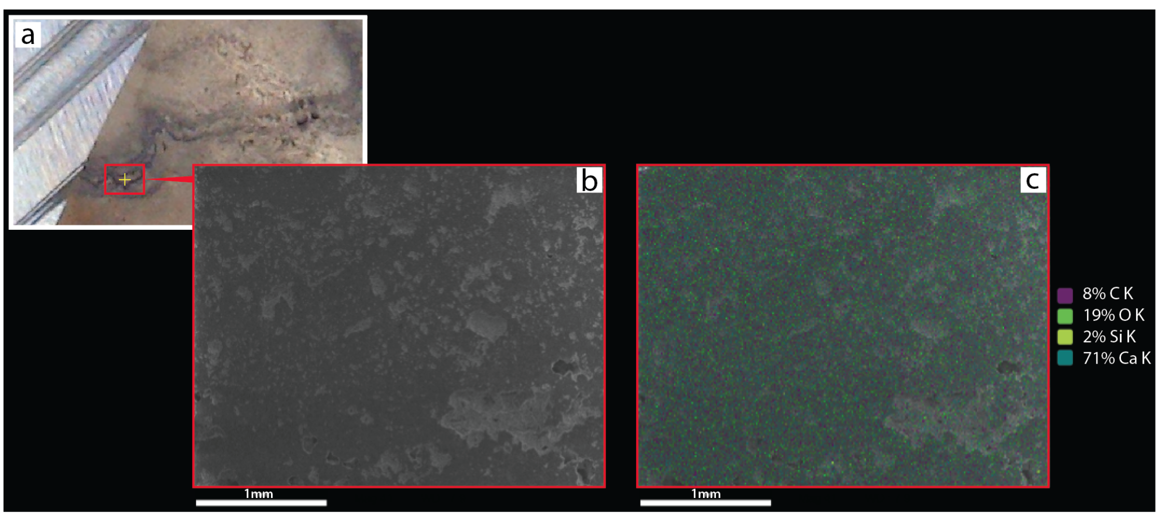

Figure S2. EDX analysis of the Orgnac 3 speleothem (Org3-fsp1). (a) Location of the region used for elemental mapping; (b) polished section (1 µm grain); and (c) synthetic map with measured elements (Ca, O, C, Si; above detection limits) overlain on a SEM image of the analyzed area. Identification of black deposits as soot films is suggested by the black color and the exclusion of the metallic oxides. Bar scale: 1 mm.

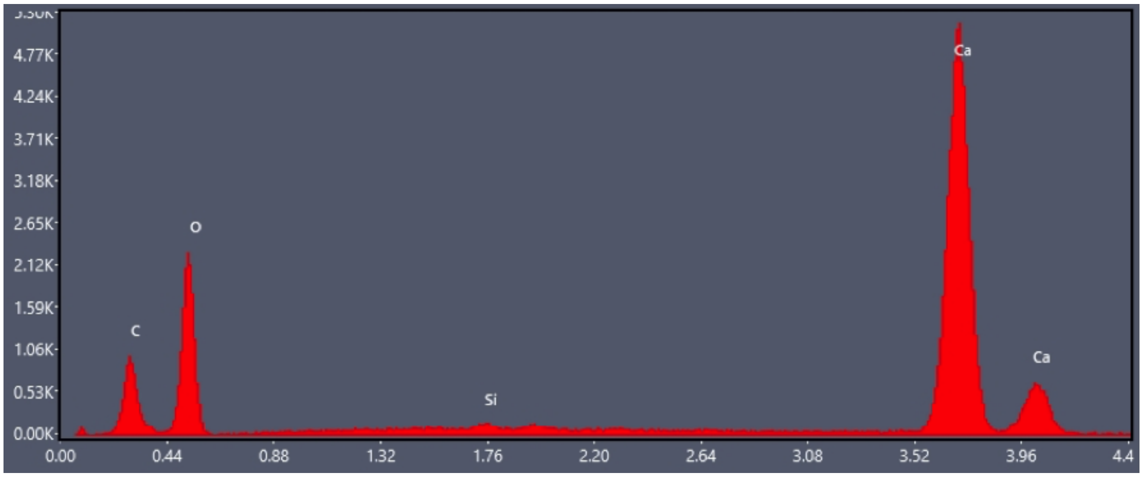

Figure S3. EDX spectrum of the analyzed area (Figure S2). This area includes at least two obvious black layers. Four distinct principal peaks (I> 0.5K) are visible in the EDX spectrum. From left to right: CK: 0.277keV, OK: 0.525 keV, CaKα1: 3.692 keV, and CaKβ: 4.013keV. The description of Si (for an energy of about 1.739 keV) can be retained (although it is not statistically significant). Settings are kV: 20; Mag: 41; Takeoff: 33.02; Live time: 112.5376; Amp time (µs): 3.84; Resolution (eV): 129.5; Det: Element-C2B.

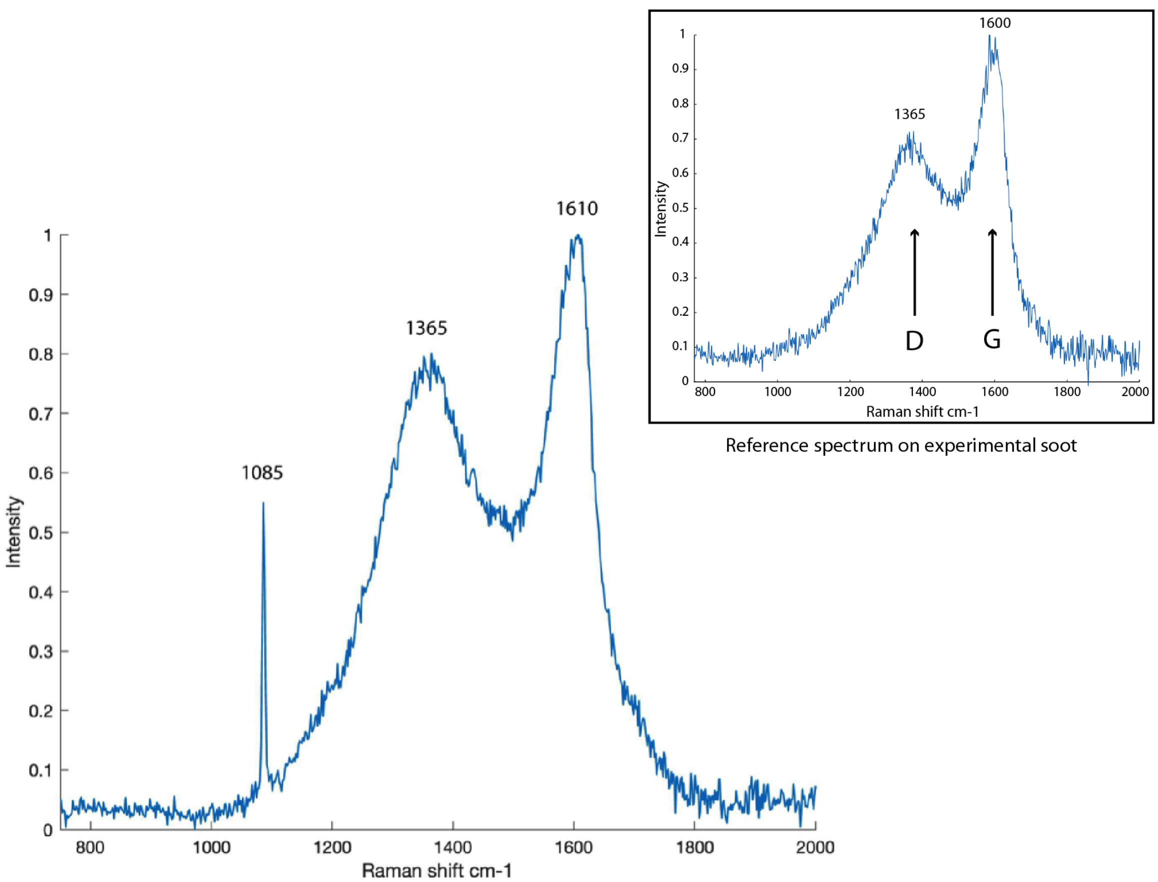

Figure S4. Raman spectrum recorded on a black layer from Org3-fsp1 (514 nm laser, 5% laser intensity; 2.5 mW, 30 s time exposure, 6 accumulations). The fluorescence signal was subtracted with a linear baseline or quadratic function when significant. The first peak at 1085 cm^{-1} is characteristic of calcite. D and G carbon bands, typical of carbon materials, are observed respectively around 1365 and 1610 cm^{-1}. Their shape (relative intensity and width) is typical for strongly defective carbonaceous materials and confirms the identification of soot. Inset figure: the obtained spectrum on experimental soot (produced by wood combustion) can serve as a reference to confirm soot identification. This spectrum also confirms the very good preservation of soot (a signal that can still be identified at least 250 ky after its formation).

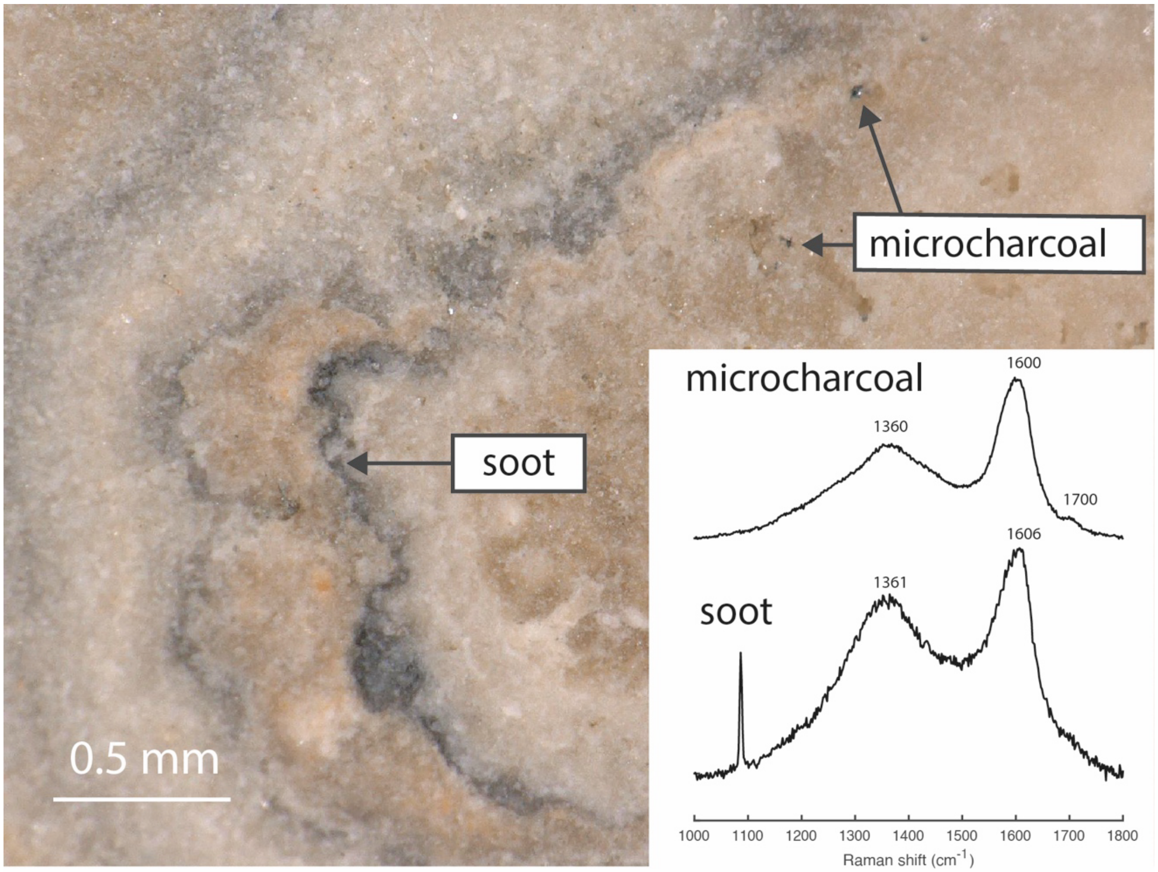

Figure S5. A Raman spectrum (bottom spectrum) recorded from a black layer from Org3-fsp1, characterized as soot according to the two Gaussian-shaped bands (D and G). A Raman spectrum recorded on black particles from Org3-fsp1, characterized as microcharcoals, with multiple shoulders and, in particular, the band at 1700 cm^{-1} (see Deldicque et al. 2023). Note that some micro-charcoals are not directly associated with soot bands. It can be due to polishing process, the sample's high porosity possibly favoring the trapping of microcharcoal (coming from black bands) in asperities. They can also have been displaced by percolation, since they are larger than the soot nanoparticles that stain the calcite forming soot films marking fire events. On the contrary, soot particles that do not create "ghost soot films" resulting from re-deposition during calcite growth, as shown by experiments – Vandevelde et al. 2023).

Supplementary Note 4 – Construction of the soot-film chronology

Sample preparation and observation As per the protocol developed by Vandevelde et al. (2017), the sections were polished with 500 FEPA (12.8 µm grain size) free grains for observation and a diamond gel (up to 1 µm grain size) for characterization analyzes (Supplementary Note 3). A thin section was also prepared by Christophe Nevado (Géosciences Montpellier) to observe the crystalline fabric of Org3-fsp1-s1 after its study as a polished section. The large dimensions of the thin section (9 × 15 cm) allowed us to study the sample in one piece, without the need for reassembling different areas or losing observation areas because of the saw cuts.

We constructed the chronology by comparing the observation of Org3-fsp1-s1 with other polished sections to ensure the proper identification of each soot film or package of soot films. This section (Org3-fsp1-s1) was also studied as a thin section. Some films that were uncertain or unclear in thin section were clearly identified in the polished section, such as the 13th film from the base of the speleothem. Therefore, it was included as a certain soot film in the final chronology presented in Figure 3 (Main text). However, difficulties in observing it in transmission light on the thin section prevented us from determining its position relative to the calcite crystalline fabric (see below).

The entire chronology was constructed by combining data from microscopic photographs (Figures S6 and S7). All observations were then verified and validated under the microscope.

Recording the position of soot films within the calcite crystalline fabric The Org3-fsp1 carbonated formation exhibited laminated structure with three types of crystalline fabrics: sparite (large calcite crystals >10 µm), micro-sparite (calcite crystals between 5 and 10 µm), and micrite (small calcite crystals <5 µm). Sparite was found exclusively in the fissures of the speleothem, indicating subsequent precipitation. Thin-section observations allowed differentiating between (micro-)sparite and micrite (Figure S8).

The type of crystalline fabric depends on various factors (identified by Frisia et al. (2000) and references therein). The microcrystalline fabric observed in Org3-fsp1 forms under near-equilibrium conditions (low supersaturation of the parent solution) and during highly fluctuating flow rates of seepage water. The presence of growth inhibitors, detrital and colloidal particles associated with major seepage events, can promote the development of this fabric (Frisia et al. 2000). The visible lamination of speleothems is primarily influenced by hydrological variations (Baker et al. 2008; Fairchild et al. 2000; Frisia and Borsato 2010). Periods of excess water supply lead to the precipitation of calcite as (micro-)sparitic laminae, appearing dark in reflected light (DCL – dark compact laminae); these represent high-flow periods with reduced water residence time in the soil, epikarst, and karst. During drier phases, calcite precipitates as micritic laminae, composed of smaller calcite crystals appearing white in reflected light (WPL – white porous laminae); this indicates lower flow rates and increased water residence time (Fairchild et al. 2000; Genty and Deflandre 1998; Genty and Quinif 1996).

In transmission light, sparite appears translucent, and micrite appears dark. Soot is opaque and black in both transmission and incident light. The combination of reflected and transmitted light enables the differentiation of calcite doublets and soot films. Under these conditions, micro-sparite appears semi-translucent, micrite appears whitish and/or opaque, and soot films are the only dark elements (Figs. S6 and S7). These observation conditions enable the documentation of the relationship between soot films and the calcite micrite/micro-sparite alternation.

In areas where the lamination is less clear, we focused on documenting the position of soot films in preserved sections with the clearest position. To account for the various parameters and increased uncertainties, we calculated confidence scores (*cf.* Supplementary Note 6).

Observations and microphotographs of the Org-fsp1-s1 thin section were conducted using a Nikon Eclipse E600 POL polarizing microscope coupled with a Leica Schott KL 1500 fiber-optic light source at the MAPS Platform of MSH Mondes (USR 3225 CNRS, Nanterre, France).

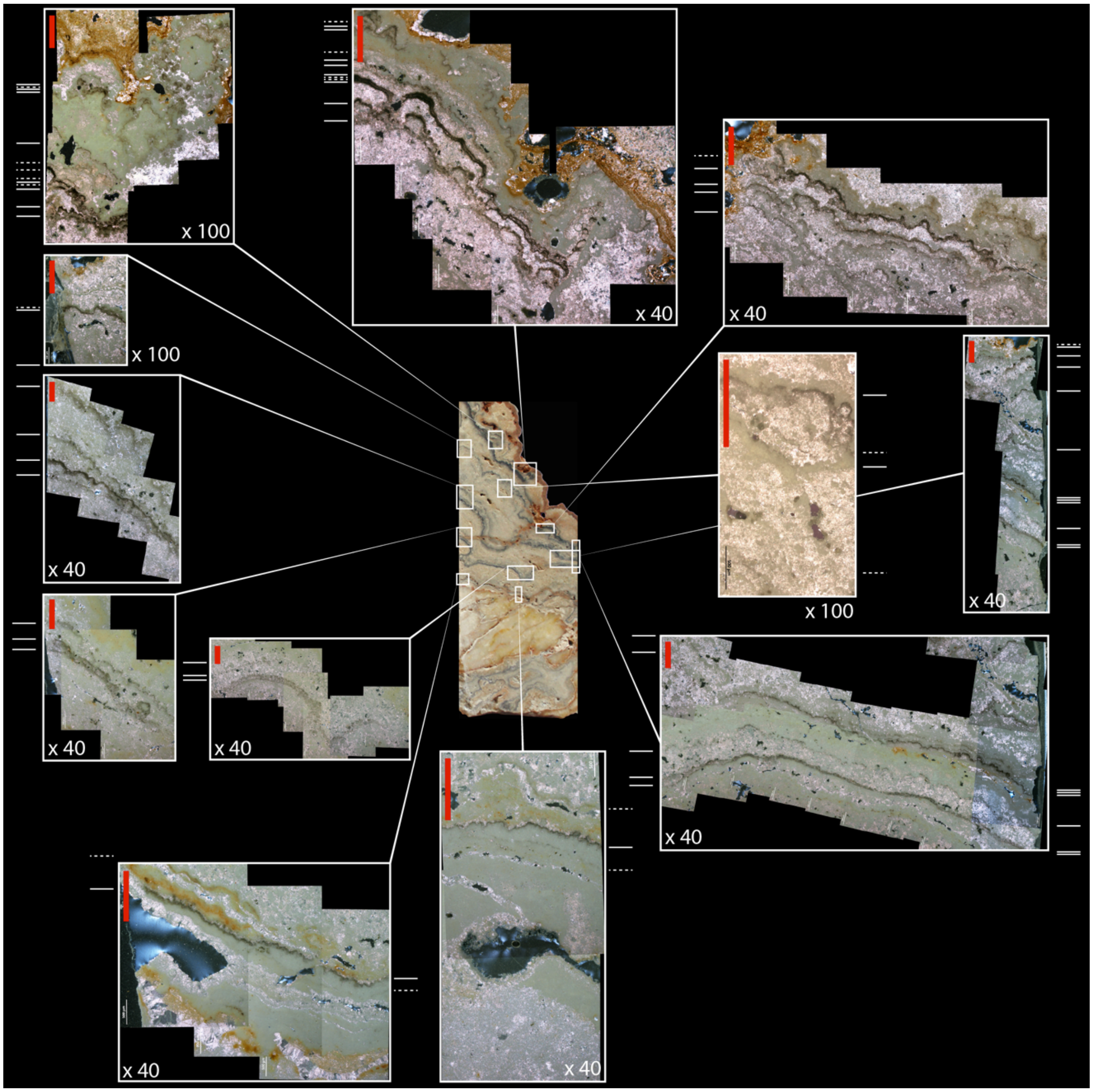

Figure S6. Combining data collected from different areas on Org3-fsp1-s1. The barcodes next to the pictures (×40 or ×100 magnification, crossed-polarized transmitted light coupled with reflected light – XPL + RL) represent the soot-film succession documented at the locations indicated by the white squares. Each line represents a soot film; dotted lines represent possible soot films. 1 mm scale in red. See Figure 3 in the main text for the synthesis of barcode synchronization.

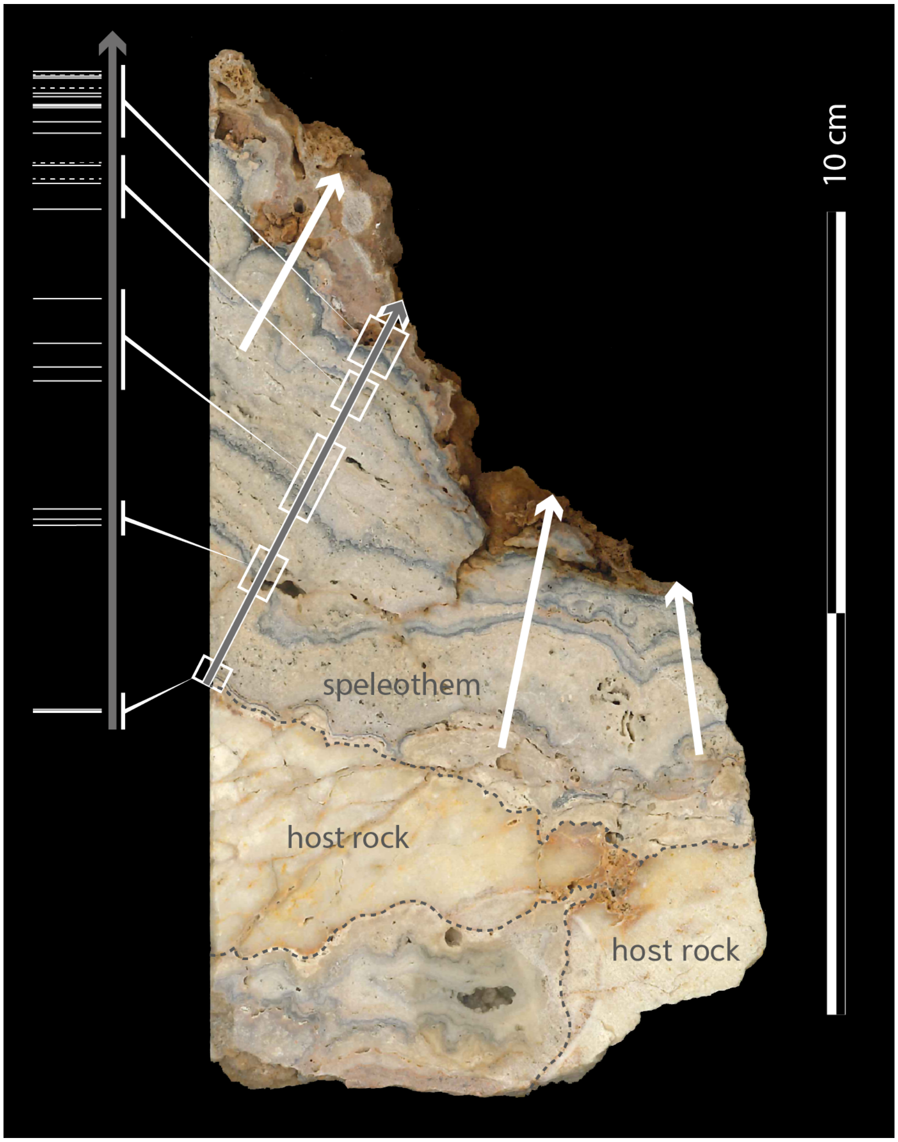

Figure S7. Paleo-fire chronicle with succession of soot films recorded on the gray transect. The arrows on the speleothem indicate the growth axes. The soot films are not uniformly distributed: five distinct zones of soot film concentration have been documented. These five distinct zones of soot accumulation are indicated by the white squares. Some soot films appear stacked on this figure. In Figure 3 (main text) the five soot films packages are extended at different scales to show all the soot films.

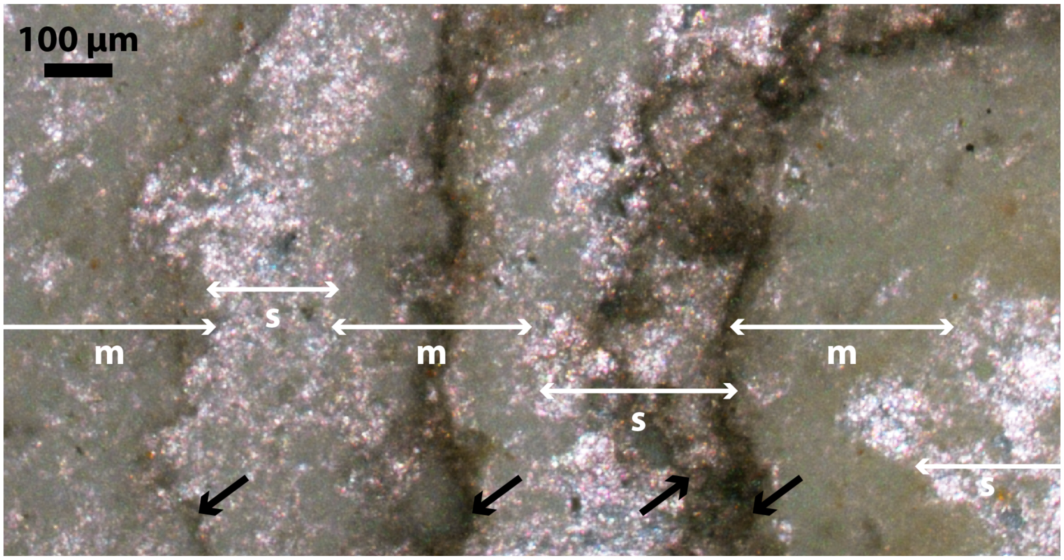

Figure S8. Observation of crystalline fabric and soot films in crossed-polarized transmitted light coupled with reflected light (XPL + RL); m: micrite, s: (micro-)sparite, black arrows: soot films. We see, particularly on the right side of figure, that the presence of soot can prevent the clear identification of the crystalline fabric. To overcome this, we adjusted the observation settings by increasing the power of the transmitted light or of the reflected light. The position of soot films in the micrite/micro-sparite alternation is sometimes less clear than in this figure; we therefore calculated a confidence score to quantify the degree of uncertainty in the data (Supplementary Note 6).

Supplementary Note 5 – U-Th dating

Stratigraphic sampling for dating was performed on Org3-fsp1-s2, a section adjacent and parallel to Section 1, which supported the reconstruction of the fire event chronology. This allowed us to sample sufficient material (between 50 and 160 mg of calcite) without damaging the Org3-fsp1-s1 reference section while still being able to study it in thin section. Using packages of soot films as reference horizons facilitated establishing the correspondence between the two sections (Org3-fsp1-s1 and Org3-fsp1-s2) (Figure S9).

The thin section, made parallel to Org3-fsp1-s2, confirmed that no sampling was done in areas with observed alterations. Alterations were limited in extent, and corrosion was only visible on the external part of the speleothem and along cracks. Microorganisms may have played a role in the observed localized alteration processes (Suchý et al. 2021).

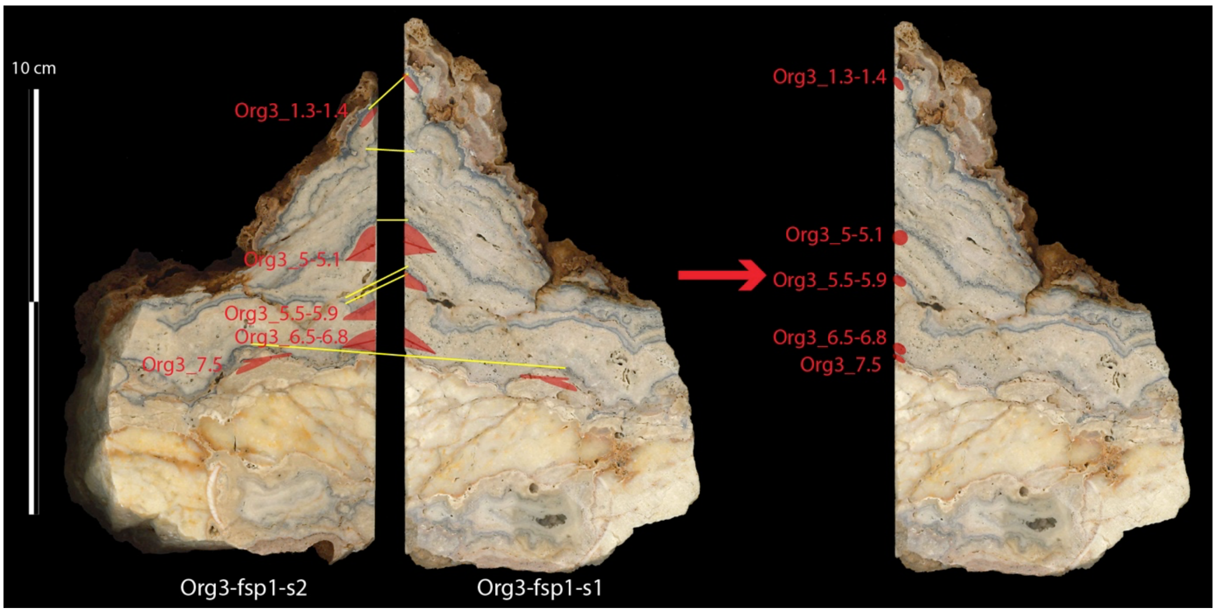

Figure S9. Synchronization of Org3-fsp1-s2 (left image) with Org3-fsp1-s1 (right image) by using soot films as reference horizons (yellow lines), and transfer of the U-Th sampling locations (in red) to Section 1.

Supplementary Note 6 – Position of soot films and calculation of confidence scores

Our observations of the Org3-fsp1 speleothem include some uncertainties, which we address using a simplified form of many-valued logic (or Łukasiewicz logic). This non-classical logic entails using intermediate values between false (0) and true (1) to express greater or lesser uncertainty. It can be seen as a discretization of fuzzy logic, which allows for an infinite number of values between true and false (Bernadet 2011). In this case, these intermediate values, referred to as "truth fractions," are associated with uncertain observations and are used to compute scores.

The first uncertainty in our data set is the presence of the observed soot film, which is either relatively easy or challenging to observe (thin, short, fuzzy, or discontinuous). On the barcode diagrams (Figures 3 and S6) the certain soot films are represented by solid lines, and the uncertain soot films are indicated by dotted lines. An "existence score" (A score) can be assigned to each soot film to formalize this uncertainty and incorporate it into further calculations. We have defined two “certainty” values:

- soot film = 1 (exists)
- uncertain soot film = 1⁄2 (may exist, or not)

The second uncertainty concerns the location of each soot film vis-à-vis the calcite crystalline fabric. From our observations, we set a “location accuracy score” (B score) with five “certainty”-values indicating whether the position is:

- certain = 1 (soot film is associated with micrite or sparite)
- almost certain = 9⁄10
- very probable = 4⁄5
- probable = 3⁄4
- uncertain = 1⁄2 (complete uncertainty: soot film can be associated equally with micrite and sparite)

To determine the reliability of each soot film's association with micrite or sparite, we multiplied the existence score (A score) by the B score to derive a "confidence score." The mean value of the individual confidence scores represents the confidence score for the entire data set.

In Table S1, the position of soot films in the calcite crystalline fabric is reported for 23 out of 27 films. Among these films, the three at the top of the speleothem are associated with white porous calcite (WPC) without clear laminations. The 13th film, in chronological order from the bottom, has an indeterminate position depending on the areas where it is observed. These four films are equally likely to be associated with micrite (WPL) or (micro-)sparite (DCL).

Observations of the location of soot films in the calcite crystalline fabric show that 48% of soot films were associated with micritic laminae (WPL), whereas 52% were associated with sparitic deposits (DCL). Considering all the soot films of the chronology, including those with unknown positions, the confidence score was 5/6 (Table S2). However, when considering only the films with known positions (excluding the four films with complete uncertainty), the confidence score increased to 9/10 (Table S3).

Table S2. Calculation of Confidence Score about soot films position in calcite crystalline fabric. Taking into account all the soot films of the chronology, including those for which we have no information about their position regarding DCL or WPL.

Soot film (in chronological order from bottom to top)	Position of soot film in crystalline fabric of calcite				**Confidence score** *(A score x B score)*
	A score (soot film existence score)	**Association with WPL**	**Association with DCL**	**B score** (location accuracy score)	
27	1	1/2	1/2	1/2	1/2
26	1/2	1/2	1/2	1/2	1/4
25	1	1/2	1/2	1/2	1/2
24	1	1		1	1
23	1/2		1	1	1/2
22	1		1	9/10	9/10
21	1		1	1	1
20	1		1	3/4	3/4
19	1	1		3/4	3/4
18	1		1	1	1
17	1	1		1	1
16	1		1	1	1
15	1/2	1		1	1/2
14	1		1	1	1
13	1/2	1/2	1/2	1/2	1/4
12	1	1		1	1
11	1		1	1	1
10	1	1		3/4	3/4
9	1	1		1	1
8	1	1		1	1
7	1		1	9/10	9/10
6	1		1	1	1
5	1		1	1	1
4	1	1		1	1
3	1		1	4/5	4/5
2	1	1		1	1
1	1	1		1	1
Total		**13**	**14**		**5/6**
***N* = 27**		**48%**	**52%**		

Table S3. Calculation of the confidence score for soot-film position within the calcite crystalline fabric. The calculation accounts only for the soot films of the chronology for which we have information about their position in relation to DCL or WPL (the four soot films lacking information were excluded).

Soot film (in chronological order from bottom to top)	Position of soot film in crystalline fabric of calcite				
	A score (soot film existence score)	**Association with WPL**	**Association with DCL**	**B score** (location accuracy score)	**Confidence score** *(A score x B score)*
27	-	-	-	-	-
26	-	-	-	-	-
25	-	-	-	-	-
24	1	1		1	1
23	1/2		1	1	1/2
22	1		1	9/10	9/10
21	1		1	1	1
20	1		1	3/4	3/4
19	1	1		3/4	3/4
18	1		1	1	1
17	1	1		1	1
16	1		1	1	1
15	1/2	1		1	1/2
14	1		1	1	1
13	-	-	-	-	-
12	1	1		1	1
11	1		1	1	1
10	1	1		3/4	3/4
9	1	1		1	1
8	1	1		1	1
7	1		1	9/10	9/10
6	1		1	1	1
5	1		1	1	1
4	1	1		1	1
3	1		1	4/5	4/5
2	1	1		1	1
1	1	1		1	1
Total		**11**	**12**		**9/10**
***N* = 23**		**48%**	**52%**		

Supplementary Note 7 – LA-ICP-MS analysis

LA-ICP-MS analysis was conducted at LabMaTer (UQAC, Canada) using a RESOlution 193 nm laser ablation system equipped with a double-volume cell (S155, Laurin Technic), coupled to an Agilent ICP-MS (7900). A circular beam size of 33 µm was used with a scan speed of 20 µm/s, a fluence of 5 J/cm^2, and a pulsing rate at 25 Hz to produce data points approximately every 6–7 µm. Calibration relied on two NIST-glasses (610 & 612) and two USGS-basaltic glasses (GSD-1g & GSE-1g). Quality control monitoring involved analyzing NIST-614 and 616, as well as two carbonate pressed pellets (USGS-MACS-3 and USGS-GProbe-4) (see Figure S10). For the glasses and GProbe-4, calcium (^{44}Ca) the internal standard, whereas normalization was used for the line scan and MACS-3 given the absence of a fixed internal standard for unknown-heterogeneous samples. Calcite stoichiometry ($CaCO_3$) dictated the normalization to 56% using CaO, Al_2O_3, SiO_2, MnO, FeO, and MgO to compensate for the 44% CO_2 that LA-ICP-MS cannot quantify. In cases where small silicate inclusions were detected in the transects, we slightly modified the quantification method to force normalization to 100%. The new IOLITE "3D-data reduction scheme" (described in Paul et al.–2023) was used for this purpose.

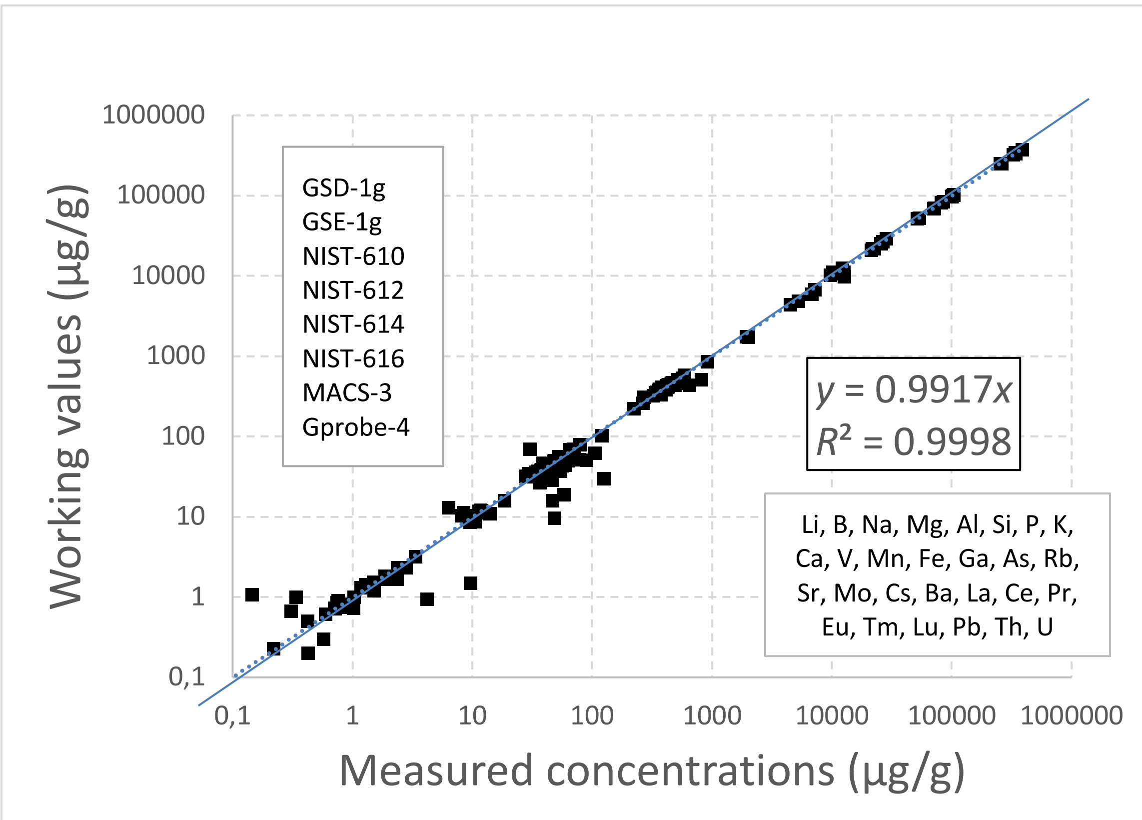

Figure S10. Quality assessment of LA-ICP-MS comparing the measured data of the reference material with their working values. As underlined by Savard et al. (2023), discrepancies can arise from the heterogeneity and/or the poor characterization of the material.

Supplementary Note 8 – Counting annual cycles

These data were used to construct annually resolved chronologies from the trace element data by converting depth to time. The data were smoothed using a simple moving average with a window size of 10 to reduce noise. We used the 'find_peaks' algorithm from the scipy signal processing library to identify significant concentrations of chemical elements in each scan. To estimate the annual cycles, we counted the total number of positive peaks in scans 3 and 4. A key part of our methodology involved managing the overlap between successive scans in the time series. We subtracted the number of peaks at the beginning of scan 4 (which was less reliable because of the greater porosity) from the total number of peaks (i.e., Scan 3 + Scan 4 − Overlap zone). Table S4 summarizes the peaks computed from the ^{88}Sr, ^{138}Ba, ^{24}Mg, and ^{238}U ppm time series.

Positive peaks observed	Sr88	Ba138	Mg24	U238
Scan 3 + Scan 4	1016	1123	1059	1223
Estimated overlap region	101	86	92	104
Scans 3 + Scan 4 − Overlap	**915**	**1037**	**967**	**1119**

Table S4. Positive peaks detected from each time series of Scan 3 and Scan 4. Peaks are detected post-preprocessing using a simple moving average with a sliding window of size 10.

To ensure that real peaks were being counted and did not represent artifacts, we verified whether the small peaks existed for one chemical element and also for the other chemical elements. We standardized the data using 'StandardScaler' from 'Scikit-learn,' which is analogous to the application of z-score standardization, to directly compare the concentration variations between the various elements (Figure S11). The resulting graphs clearly illustrate the temporal correlation of concentration variations, confirming that sometimes-unclear variations on a single element can be confirmed by comparing with other elements that exhibit annual cyclicity. Observing multiple elements simultaneously helped to limit data uncertainty, which was estimated at 4%–7% when using a single element like Sr to document annual cycles compared to an uncertainty of 2% when studying at least three elements (Sr, Ba, and U) simultaneously (Nagra et al. 2017a).

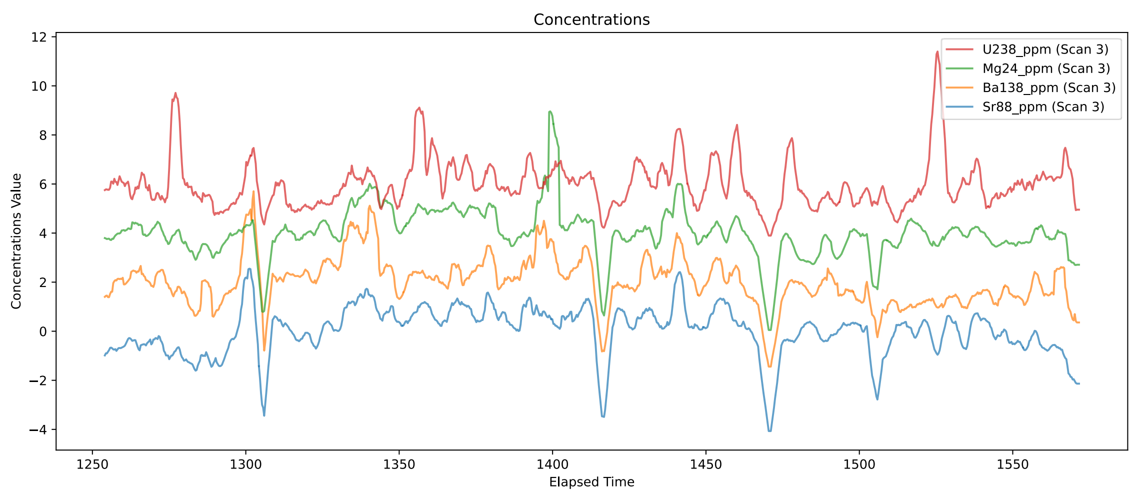

Figure S11. Comparison of the standardized concentration of four elements (U, Mg, Ba, Sr) placed on the same standardized scale using StandardScaler (z-score). The observation zone was extracted from the entire cycle displayed in Figure S12.

Because of the high porosity of the Org3-fsp1 sample, there were gaps in the collected elemental data, which may result in missing peaks in the sequence. The variations in U were slightly more numerous than those for Mg, Sr, and Ba, suggesting possible artifact counting given the low concentration of measured U (and therefore perhaps slightly noisier data). The Ba concentration was lower than that of Sr and Mg, resulting in slightly higher peak numbers, likely for the same reasons. To estimate the number of annual cycles recorded in the Org3-fsp1 speleothem, we averaged the data for all four elements. However, it should be noted that the data for U (and Ba) may be slightly overestimated, whereas the data for the other elements may be underestimated because of missing peaks when considering only one element at a time. Consequently, the uncertainty in the data for this type of speleothem is likely greater than the 2%–4% achieved by Nagra et al. (2017). Nevertheless, our approach still provides a more accurate view of the speleothem's growth time than relying solely on direct radiometric dating. Figure S11 illustrates the complete cycle for Sr (scans 3 and 4 without overlapping).

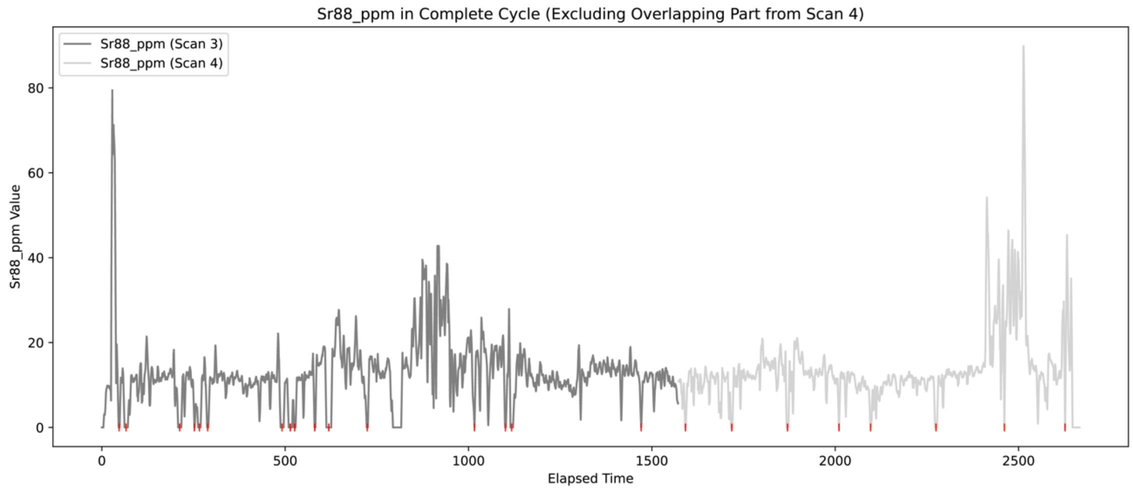

Figure S12. Complete cycle for Sr, excluding the overlapping section. The red lines indicate porosity.

Supplementary Note 9 – UV fluorescence

UV fluorescence analysis was carried out on the Org3-fsp1-s4 section. Fluorescence wavelength relates to the composition of the dissolved organic matter (Baker et al. 1998; Perrette et al. 2005). The mean fluorescence spectrum obtained from the Org3-fsp1 speleothem (Figure S13) showed a shoulder in the fluorescence spectrum, which is associated with aromatic amino compounds. This shoulder is likely indicative of organic compounds and microbial laminae within the speleothem.

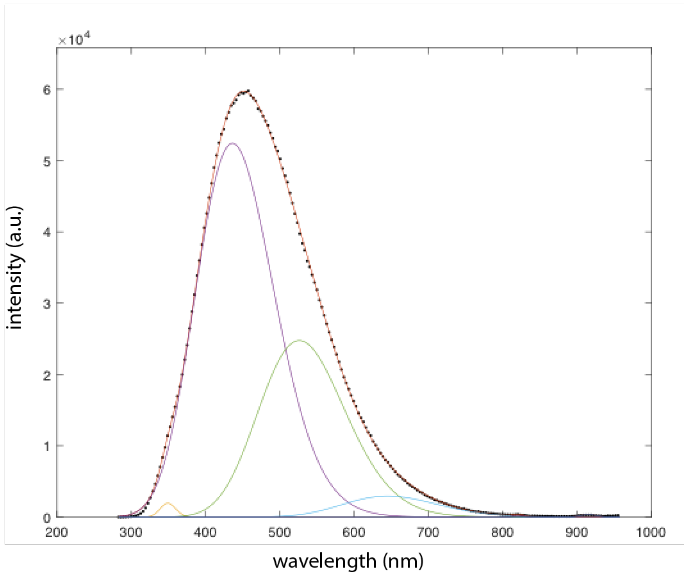

Figure S13. Fluorescence spectrum of mean emissions with the simulation of protein-like (yellow) fulvic-like (purple), humid-like (green) fluorophores, and Mn substituted into the calcite lattice (blue). Data was acquired along transects over the full length of Org-fsp1-s4 speleothem.

The most probable source of fluorescence in stalagmites is dissolved organic matter. Annual fluorescent laminae are formed as a result of the transfer of fluorescent material from the overlying soil to the stalagmite. The seasonal variation in fluorescence intensity is influenced by the climatic conditions, such as monsoons in Southeast Asia or the resumption of rainfall during autumn in temperate areas. These climate changes lead to an increase in dissolved organic matter because of an increase in discharge (Baker et al. 2008). The counting of these annual fluorescent laminae can be used to determine the duration of speleothem formation. In this study, the unfiltered fluorescent intensity acquired from six scans on the Org-fsp1-s4 speleothem was used for laminae counting (Figure S14). The count of fluorescent laminae was 914 ± 10, which closely aligned with the 915 cycles counted for variations in Sr concentration on the Org3-fsp1-s1 section. This finding confirmed the annual cycle count based on trace elements.

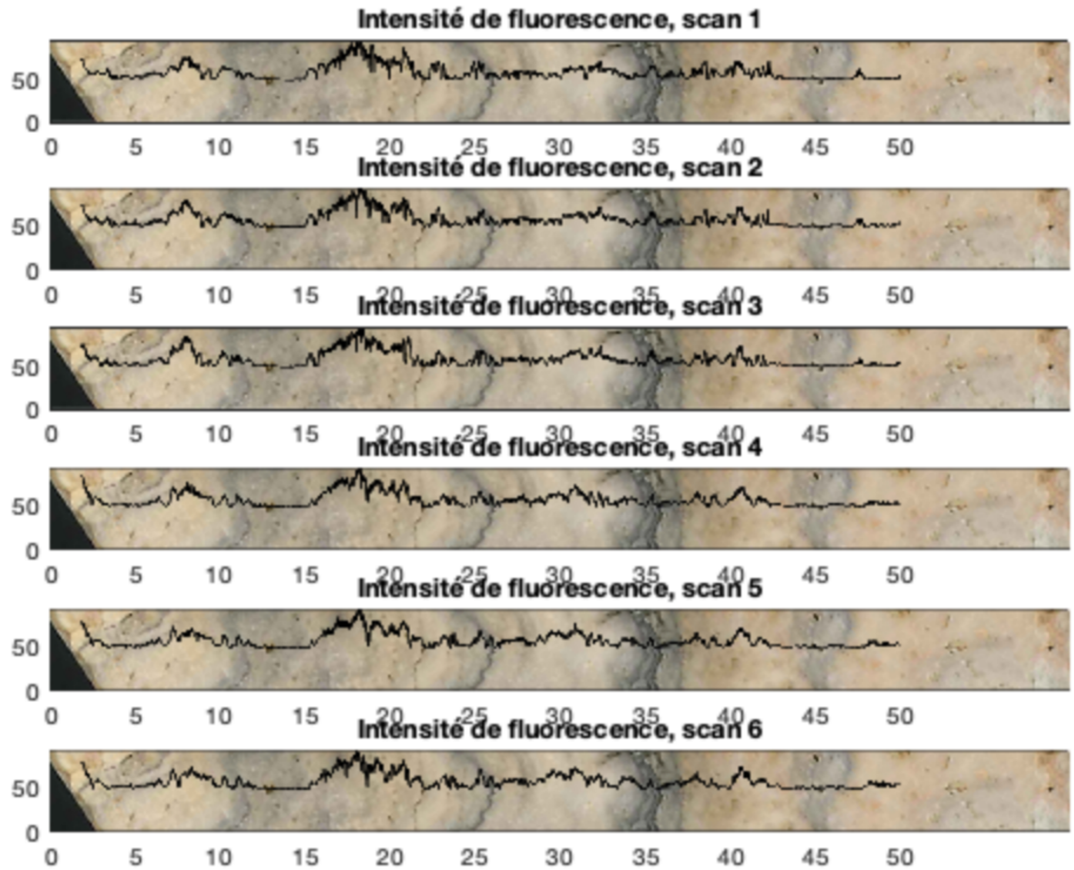

Figure S14. Unfiltered fluorescent intensity for the six scans acquired from the Org-fsp1-s4 speleothem, used for laminae counting.

Supplementary Note 10 – Thermal alteration of archaeological material at the Orgnac 3 site

Table S5. Number of burnt lithics within each archaeological level at Orgnac 3. ns = not studied; *sampling among the lithic collection (made in the richest square meters and in the area of the Australia limestone block, *eg.* C, D and E strips).

Archaeological layer	Burnt lithics (*N*)	Total lithic pieces (*N*)	%
2	2100	8213	25.6%
3	Ns	ns	ns
4a	503	2125*	23.7%
4b	799	3070*	26.0%
5a	493	1875*	26.3%
5b	1637	4910*	33.3%
6	3023	12934	23.4%
7	93	760	12.2%

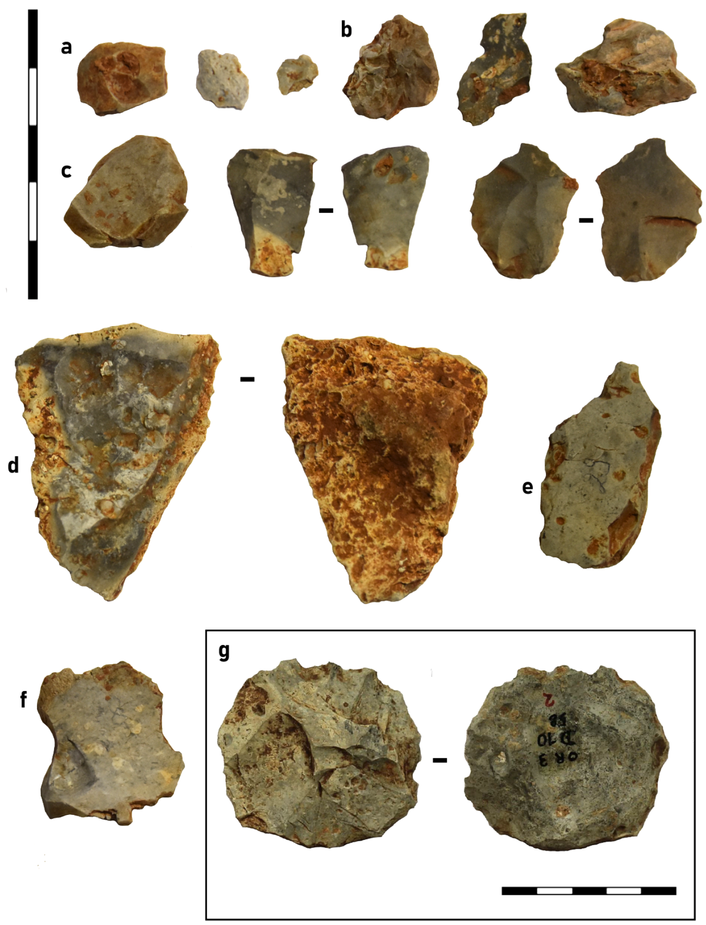

Figure S15. Examples of thermal alteration on flint. a) Thermal cupulae from level 4a; b) burnt chunks from Level 4a; c, e, f) burnt flakes from Level 4a; d) burnt cortical flake from Level 4a; g) burnt Levallois core from Level 2.

Table S6. Number of burnt bones in the archaeological levels of Orgnac 3. Data courtesy of Anne-Marie Moigne.

Archaeological layer	Burnt bones (*N*)	Total bones (*N*)	%
1	46	2375	1.94%
2	27	2551	1.06%
3	17	2057	0.83%
4a	15	406	3.69%
4b	12	563	2.13%
5a	20	854	2.34%
5b	51	1232	4.14%
6	50	1663	3.01%

Note: The percentages of heated bones are low in comparison to burnt lithics because of the material considered for each analysis. The account for the lithic materials is based on all the lithics recovered from the site, including the sieving products (by square meter and layer). This is not the case for faunal remains: only coordinated elements were studied. Coordinated elements are generally the largest or determinable elements. As fire fragments bones, it is very likely that burnt bones are over-represented in the assemblage among the sieve remains, compared with the coordinated remains. However, J. Combier mentioned heated bone concentrations (Combier, 1967).

Table S7. Observation and descriptions of combustion features for each level, made by J. Combier during the excavations. Presence/absence and type of hearth identified by J. Combier (1967) and other observations related to combustion features.

Level	**Hearth**	**Other observation**
1		
2	Traces of ancient hearths	
3	One ancient "faded" hearth	Concentration of burnt lithic and faunal remains
4a	Low traces of ancient hearths	
4b	Numerous "faded" hearths ("*foyers délavés"*)	High concentration of burnt bone and lithic remains (≃ 50 cm; E10 square); small block delimiting the hearth?
5a	Traces of ancient hearths	
5b	Central hearth, bowl-shape ("*en cuvette*")	Most of the heated lithic remains found around the hearth
6		Burnt faunal remains (only 2m² excavated)

SI References

Aldhouse-Green, S., Peterson, R., & Walker, E. A. (Eds.). (2011). *Neanderthals in Wales: Pontnewydd and the Elwy Valley Caves*. Oxbow Books. https://doi.org/10.2307/j.ctt1f5g4qb

Aranguren, B., Revedin, A., Amico, N., Cavulli, F., Giachi, G., Grimaldi, S., et al. (2018). Wooden tools and fire technology in the early Neanderthal site of Poggetti Vecchi (Italy). *Proceedings of the National Academy of Sciences of the United States of America*, *115*, 2054–2059. https://doi.org/10.1073/pnas.1716068115

Arsuaga, J. L., Fernández Peris, J., Gracia-Téllez, A., Quam, R., Carretero, J. M., Barciela González, V., et al. (2012). Fossil human remains from Bolomor Cave (Valencia, Spain). *Journal of Human Evolution*, *62*, 629–639. https://doi.org/10.1016/j.jhevol.2012.02.002

Baker, A., Genty, D., Dreybrodt, W., Barnes, W. L., Mockler, N. J., & Grapes, J. (1998). Testing theoretically predicted stalagmite growth rate with recent annually laminated samples: Implications for past stalagmite deposition. *Geochimica et Cosmochimica Acta*, *62*, 393–404. https://doi.org/10.1016/S0016-7037(97)00343-8

Baker, A., Smith, C., Jex, C., Fairchild, I., Genty, D., & Fuller, L. (2008). Annually laminated speleothems: A review. *International Journal of Speleology*, *37*, 193–206. https://doi.org/10.5038/1827-806X.37.3.4

Behm-Blancke, G. (1960). *Altsteinzeitliche Rastplaetze Im Travertingebiet von Taubach, Weimar, Ehringsdorf*. Weimar: Hermann Bohlaus Nachfolger.

Benvenuti, M., Bahain, J. J., Capalbo, C., Capretti, C., Ciani, F., D'Amico, C., et al. (2017). Paleoenvironmental context of the early Neanderthals of Poggetti Vecchi for the late middle Pleistocene of Central Italy. *Quaternary Research*, *88*, 327–344. https://doi.org/10.1017/qua.2017.51

Bernadet, M. (2011). *Introduction pratique aux logiques non classiques*. Hermann.

Bister, T. (2005). Le feu au Paléolithique ancien. *Anthropologia et Praehistorica*, *116*, 51–58.

Blasco, R. (2006). *Estrategias de subsistencia de los homínidos del Nivel XII de la Cova del Bolomor (La Valldigna, Valencia). Memoria de licenciatura. Departament d'Història, Història de l'Art i Geografia*. Universitat Rovira i Virgili.

Blasco, R., & Peris, J. F. (2009). Middle Pleistocene bird consumption at Level XI of Bolomor Cave (Valencia, Spain). *Journal of Archaeological Science*, *36*, 2213–2223. https://doi.org/10.1016/j.jas.2009.06.006

Blasco, R., Rosell, J., Sañudo, P., Gopher, A., & Barkai, R. (2016). What happens around a fire: Faunal processing sequences and spatial distribution at Qesem Cave (300 ka), Israel. *Quaternary International*, *398*, 190–209. https://doi.org/10.1016/j.quaint.2015.04.031

Boëda, E., Soriano, S., & Noël-Soriano, S. (2000). Fonction et fonctionnement d'un site à la fin du Pléistocène moyen. Le niveau acheuléen C'3 de Barbas I (Creysse, Dordogne) (pp. 293–305). Presented at the Approches fonctionnelles en Préhistoire, XXVème Congrès Préhistorique de France, Société préhistorique française.

Bonneau, A., Brock, F., Higham, T., Pearce, D. G., & Pollard, A. M. (2011). An improved pretreatment protocol for radiocarbon dating black pigments in San Rock Art. *Radiocarbon*, *53*, 419–428. https://doi.org/10.1017/S003382220003455X

Bordes, F. (1971). Observations sur l'Acheuléen des grottes en Dordogne. *Munibe*, *23*, 5–23.

Bourguignon, L., Djema, H., Bertran, P., Lahaye, C., & Guibert, P. (2008). Le gisement Saalien de Petit-Bost (Neuvic, Dordogne) à l'origine du Moustérien d'Aquitaine ? In J. Jaubert, J.-G. Bordes, & I. Ortega (Eds.), *Les sociétés du Paléolithique dans un Grand Sud-Ouest de la France : nouveaux gisements, nouveaux résultats, nouvelles méthodes* (pp. 41–55). Paris, France: Mémoire XLVII de la Société Préhistorique française.

Brenet, M., Bourguignon, L., Colonge, D., Folgado, M., Jarry, M., Lelouvier, L.-A., et al. (2014). Les techno-complexes au début du Paléolithique moyen en Aquitaine septentrionale : complexité, complémentarité des productions de débitage et de façonnage et implications comportementales. In J. Jaubert, N. Fourment, & P. Depaepe (Eds.), *Transitions, ruptures et continuité en Préhistoire, actes du XXVIIème Congrès préhistorique de France, 31 mai-5 juin 2010* (Société Préhistorique Française., pp. 81–101). Paris.

Brenet, M., Folgado, M., Lenoble, A., Bertran, P., Vieillevigne, E., & Guibert, P. (2006). Interprétation de la variabilité technologique de deux industries du Paléolithique moyen ancien du Bergeracois Cantalouette 1 et Combe Brune 3 (Creysse, Dordogne). Contexte géoarchéologique et chronologique, analyse techno-économique. In *Mémoire de la Société Préhistorique Française* (Vol. XLVII, pp. 57–81). Presented at the Les sociétés paléolithiques d'un grand Sud-Ouest : nouveaux gisements, nouvelles méthodes, nouveaux résultats. Journées de la Société Préhistorique Française., Société Préhistorique Française.

Burdukiewicz, J. M. (2021). The Lower Palaeolithic assemblages in Central Europe in stratigraphic and palaeogeographic background. *L'Anthropologie*, *125*, 102937. https://doi.org/10.1016/j.anthro.2021.102937

Callow, P. C. (1986). *La Cotte de St. Brelade 1961–1978: Excavations by C. B. M. McBurney*. Norwich, UK: Geobooks.

Cliquet, D., & Lautridou, J.-P. (2009). Les occupations humaines du Pléistocène moyen de Normandie dans leur cadre environnemental. *Quaternaire*, (vol. 20/3), 305–320. https://doi.org/10.4000/quaternaire.5226

Cliquet, D., Mercier, N., Valladas, H., Froget, L., Michel, D., Van Vliet-Lanoë, B., & Vilgrain, G. (2003). Apport de la thermoluminescence sur silex chauffes à la chronologie de site paléolithiques de Normandie : nouvelles données et interprétations [Thermoluminescence anting of burnt flints from Palaeolithic sites of Normandy recent advances]. *Quaternaire*, *14*(1), 51–64. https://doi.org/10.3406/quate.2003.1729

Combier, J. (1967). *Le Paléolithique de l'Ardèche dans son cadre paléoclimatique*. Imprimeries Delmas.

Compton, T., & Stringer, C. (2015). The morphological affinities of the Middle Pleistocene hominin teeth from Pontnewydd Cave, Wales. *Journal of Quaternary Science*, *30*, 713–730. https://doi.org/10.1002/jqs.2811

Coqueugniot, H., Liguero, D., Tillier, A.-M., & Chech, M. (1996). L'os frontal immature de La Chaise S. 15 (Abri Suard, La Chaise de Vouthon, Charente) : Phylogénie et pathologie. *Paléo, Revue d'Archéologie Préhistorique*, *8*(1), 9–17. https://doi.org/10.3406/pal.1996.903

Coutard, S., Antoine, P., Deschodt, L., Jamet, G., & Pawley, S. (2019). Stratigraphie et chronologie des formations du Pléistocène moyen récent (SIM 10-6) du Nord de la France, un cadre pour l'étude des occupations paléolithiques. In C. Montoya, J.-P. Fagnart, & J.-L. Locht (Eds.), (Vol. 1, pp. 63–90). Presented at the Préhistoire de l'Europe du Nord-Ouest : mobilité, climats et identités culturelles. 28e congrès préhistorique de France, Société Préhistorique Française. https://inrap.hal.science/hal-02876017. Accessed 28 January 2025

Coutard, S., Antoine, P., Hérisson, D., Pirson, S., Balescu, S., Forget Brisson, L., et al. (2018). La séquence loessique Pléistocène moyen à supérieur d'Etricourt-Manancourt (Picardie, France) : un enregistrement pédo-sédimentaire de référence pour les derniers 350 ka. *Quaternaire. Revue de l'Association française pour l'étude du Quaternaire*, (vol. 29/4), 311–346. https://doi.org/10.4000/quaternaire.10569

Daujeard, C., & Moncel, M. H. (2010). On Neanderthal subsistence strategies and land use: A regional focus on the Rhone Valley area in southeastern France. *Journal of Anthropological Archaeology*, *29*, 368–391. https://doi.org/10.1016/j.jaa.2010.05.002

de Lumley, H., Echassoux, A., Bailon, S., Cauche, D., de Marchi, M.-P., Desclaux, E., et al. (2004). *Le sol d'occupation acheuléen de l'unité archéostratigraphique UA 25 de La Grotte du Lazaret*. Aix-en-Provence, France: Edisud.

de Lumley, H., El Guennouni, K., Khatib, S., Michel, V., Pollet, G., & Saos, T. (2016). La maîtrise du feu sur les sols d'occupation acheuléens de Terra Amata. In H. de Lumley (Ed.), *Terra Amata (Tome V). Comportement et mode de vie des chasseurs acheuléens de Terra Amata* (pp. 43–96). Nice, France: CNRS Éditions.

de Lumley, M. A. (1976). Les Anté-néandertaliens dans le Sud. In H. de Lumley (Ed.), *La préhistoire française. Civilisations paléolithiques et mésolithiques* (pp. 547–560). Paris: CNRS.

de Lumley, M.-A. (1982). Les restes humains d'Orgnac 3. In H. de Lumley (Ed.), *Origine et évolution de l'Homme, catalogue de l'exposition du Laboratoire de Préhistoire au Musée de l'Homme* (Vol. 1). Paris: Musée de l'Homme.

Deldicque, D., Pozzi, J. P., Perrenoud, C., Falguères, C., Mahieux, G., Lartigot-Campin, A. S., & Rouzaud, J. N. (2021). Search for early traces of fire in the Caune de l'Arago at Tautavel (Eastern Pyrenees, France), combining magnetic susceptibility measurements, microscopic observations, and Raman analysis. *Comptes Rendus Geoscience*, *353*, 247–264. https://doi.org/10.5802/crgeos.66

Deldicque, D., Rouzaud, J. N., Vandevelde, S., Medina-Alcaide, M. Á., Ferrier, C., Perrenoud, C., et al. (2023). Effects of oxidative weathering on Raman spectra of charcoal and bone chars: Consequences in archaeology and paleothermometry. *Comptes Rendus Geoscience*, *355*, 1–22. https://doi.org/10.5802/crgeos.186

Deldicque, D., Rouzaud, J. N., & Velde, B. A. (2016). Raman – HRTEM study of the carbonization of wood: A new Raman-based paleothermometer dedicated to archaeometry. *Carbon*, *102*, 319–329. https://doi.org/10.1016/j.carbon.2016.02.042

Dominique Cliquet, & Jean-Pierre Lautridou. (2009). Les occupations humaines du Pléistocène moyen de Normandie dans leur cadre environnemental. *Quaternaire*, *20*(3), 305–320. https://doi.org/10.4000/quaternaire.5226

Fairchild, I. J., Borsato, A., Tooth, A. F., Frisia, S., Hawkesworth, C. J., Huang, Y., et al. (2000). Controls on trace element (Sr–Mg) compositions of carbonate cave waters: Implications for speleothem climatic records. *Chemical Geology*, *166*, 255–269. https://doi.org/10.1016/S0009-2541(99)00216-8

Faivre, J. P., Maureille, B., Bayle, P., Crevecoeur, I., Duval, M., Grün, R., et al. (2014). Middle pleistocene human remains from Tourville-la-Rivière (Normandy, France) and their archaeological context. *PLoS One*, *9*, e104111. https://doi.org/10.1371/journal.pone.0104111

Falguères, C., Yokoyama, Y., & Quaegebeur, J. P. (1988a). Datations de sédiments quaternaires par la méthode de Résonance de Spin Electronique (ESR). *L'Anthropologie*, *92*, 723–726.

Fernándes-Peris, J. (2007). *Cova Del Bolomor (Tavernes de La Valldigna, Valencia): Las industrias líticas del Pleistoceno medio en el ámbito del Mediterráneo peninsular* (Vol. Serie de Trabajos Varios 108). Valencia: Servicio de Investigación Prehistórical.

Fernández Peris, J., González, V. B., Blasco, R., Cuartero, F., Fluck, H., Sañudo, P., & Verdasco, C. (2012). The earliest evidence of hearths in Southern Europe: The case of Bolomor Cave (Valencia, Spain). *Quaternary International*, *247*, 267–277. https://doi.org/10.1016/j.quaint.2010.10.014

Foltyn, E., Foltyn, E., & Kozłowski, J. K. (2004). Early Middle Palaeolithic habitation structures from Rozumice Site C (Upper Silesia, Poland). In N. J. Conard (Ed.), *Settlement dynamics of the Middle Paleolithic and Middle Stone Age. Volume II* (Vol. 2, pp. 165–184). Tübingen: Kerns Verlag.

Foltyn, E., Kozlowski, J. K., & Maciej, W. J. (2005). Archaeology of the Lower Saalian (Older Stage, MIS8) in Upper Silesia: human settlement at the periphery of the continental ice-sheet. In N. Molines, M.-H. Moncel, & J.-L. Monnier (Eds.), *Données récentes sur les modalités de peuplement et sur le cadre chronostratigraphique, géologique et paléoanthropologique des* *industries du Paléolithique inférieur et moyen en Europe. BAR International Series S1364* (pp. 329–349). Oxford: Archaeopress.

Frisia, S., & Borsato, A. (2010). Karst. In A. M. Alonso-Zarza & L. H. Tanner (Eds.), *Carbonates in continental settings: Facies, environments, and processes* (Vol. 61, pp. 269–318). Elsevier.

Frisia, S., Borsato, A., Fairchild, I. J., & McDermott, F. (2000). Calcite fabrics, growth mechanisms, and environments of formation in speleothems from the Italian Alps and southwestern Ireland. *Journal of Sedimentary Research*, *70*, 1183–1196. https://doi.org/10.1306/022900701183

Gaillard, C. (1979). *L'industrie lithique du Paléolithique inférieur et moyen de la grotte de Coupe-Gorge à Montmaurin (Haute Garonne)*.

Genty, D., & Deflandre, G. (1998). Drip flow variations under a stalactite of the Père Noël cave (Belgium). Evidence of seasonal variations and air pressure constraints. *Journal of Hydrology (Amsterdam)*, *211*, 208–232. https://doi.org/10.1016/S0022-1694(98)00235-2

Genty, D., & Quinif, Y. (1996). Annually laminated sequences in the internal structure of some belgian stalagmites - importance for paleoclimatology. *Journal of Sedimentary Research*, *66*, 275–288.

Gowlett, J. A. J. (2006). The early settlement of northern Europe: Fire history in the context of climate change and the social brain. *Comptes Rendus. Palévol*, *5*, 299–310. https://doi.org/10.1016/j.crpv.2005.10.008

Gowlett, J. A. J., Hallos, J., Hounsell, S., Brant, V., & Debenham, N. (2005). Beeches Pit: Archaeology, assemblage dynamics and early fire history of a Middle Pleistocene site in East Anglia, UK. *Eurasian Prehistory*, *3*(2), 3–38.

Gradziński, M., Hercman, H., Nowak, M., & Bella, P. (2007). Age of black coloured laminae within speleothems from Domica Cave and its significance for dating of prehistoric human settlement. *Geochronometria*, *28*, 39–45. https://doi.org/10.2478/v10003-007-0029-7

Green, H. S., Stringer, C. B., Collcutt, S. N., Currant, A. P., Huxtable, J., Schwarcz, H. P., et al. (1981). Pontnewydd Cave in Wales—A new Middle Pleistocene hominid site. *Nature*, *294*, 707–713. https://doi.org/10.1038/294707a0

Guipert, G., de Lumley, M. A., Tuffreau, A., & Mafart, B. (2011). A late Middle Pleistocene hominid: Biache-Saint-Vaast 2, North France. *Comptes Rendus. Palévol*, *10*, 21–33. https://doi.org/10.1016/j.crpv.2010.10.006

Harvati, K., Röding, C., Bosman, A. M., Karakostis, F. A., Grün, R., Stringer, C., et al. (2019). Apidima Cave fossils provide earliest evidence of Homo sapiens in Eurasia. *Nature*, *571*, 500–504. https://doi.org/10.1038/s41586-019-1376-z

Hérisson, D., Airvaux, J., Lenoble, A., Richter, D., Claud, É., & Primault, J. (2012). Le gisement acheuléen de La Grande Vallée à Colombiers (Vienne, France) : stratigraphie, processus de formation, datations préliminaires et industries lithiques. *PALEO. Revue d'archéologie préhistorique*, (23), 137–154. https://doi.org/10.4000/paleo.2329

Hérisson, D., Coutard, S., Goval, E., Locht, J.-L., Antoine, P., Chantreau, Y., & Debenham, N. (2016). A new key-site for the end of Lower Palaeolithic and the onset of Middle Palaeolithic at Etricourt-Manancourt (Somme, France). *Quaternary International*, *409*, 73–91. https://doi.org/10.1016/j.quaint.2016.01.055

Hérisson, D., Locht, J. L., Auguste, P., & Tuffreau, A. (2013). Néandertal et le feu au Paléolithique moyen ancien. Tour d'horizon des traces de son utilisation dans le Nord de la France. *L'Anthropologie*, *117*, 541–578. https://doi.org/10.1016/j.anthro.2013.10.002

Jacobs, Z., Jankowski, N. R., Dibble, H. L., Goldberg, P., McPherron, S. J., Sandgathe, D., & Soressi, M. (2016). The age of three Middle Palaeolithic sites: Single-grain optically stimulated luminescence chronologies for Pech de l'Azé I, II and IV in France. *Journal of Human Evolution*, *95*, 80–103. https://doi.org/10.1016/j.jhevol.2016.03.010

Jarry, M., Bertran, P., Colonge, D., Lelouvier, L.-A., & Mourre, V. (2001). Le gisement paléolithique moyen ancien des Bosses à Lamagdelaine (Lot, France) (pp. 177–185). Presented at the Actes du XIVeme Congrès UISPP, BAR International Series 1239, 2004.
Jarry, M., Colonge, D., Lelouvier, L.-A., & Mourre, V. (2007). *Les Bosses 1, Lamagdelaine (Lot) : un gisement paléolithique moyen antérieur à l'avant-dernier Interglaciaire sur la moyenne terrasse du Lot* (Société Préhistorique Française).
Jaubert, J., Verheyden, S., Genty, D., Soulier, M., Cheng, H., Blamart, D., et al. (2016). Early Neanderthal constructions deep in Bruniquel Cave in southwestern France. *Nature*, *534*, 111–114. https://doi.org/10.1038/nature18291
Karkanas, P., Shahack-Gross, R., Ayalon, A., Bar-Matthews, M., Barkai, R., Frumkin, A., et al. (2007). Evidence for habitual use of fire at the end of the Lower Paleolithic: Site-formation processes at Qesem Cave, Israel. *Journal of Human Evolution*, *53*, 197–212. https://doi.org/10.1016/j.jhevol.2007.04.002
Kolen, J. (1999). Hominids without homes. On the nature of middle palaeolithic settlement in europe. In W. Roebroeks & C. Gamble (Eds.), *The Middle Palaeolithic occupation of Europe* (pp. 139–177). Leiden: Leiden University/European Science Foundation.
Lamotte, A., Deschodt, L., Antoine, P., Guerlin, O., & Debenham, N. (2019). Le gisement acheuléen en contexte de doline de Revelles (Somme, France) et ses caractéristiques communes à l'Acheuléen méridional. *L'Anthropologie*, *123*(4), 695–723. https://doi.org/10.1016/j.anthro.2019.102732
Lebel, S., Courty, M. A., & Rimmer, S. M. (2007a). Early Neanderthal evidence for the use of fire (OIS6-7); the remarkable archaeological and micromorphological record at the Bau de l'Aubesier rock shelter (Vaucluse, France). *Quaternary International*, *167*, 167–168.
Lebel, S., & Trinkaus, E. (2002). Middle Pleistocene human remains from the Bau de l'Aubesier. *Journal of Human Evolution*, *43*, 659–685. https://doi.org/10.1006/jhev.2002.0598
Lebel, S., Trinkaus, E., Faure, M., Fernandez, P., Guérin, C., Richter, D., et al. (2001). Comparative morphology and paleobiology of Middle Pleistocene human remains from the Bau de l'Aubesier, Vaucluse, France. *Proceedings of the National Academy of Sciences of the United States of America*, *98*, 11097–11102. https://doi.org/10.1073/pnas.181353998
Locht, J. L., Antoine, P., Hérisson, D., Gadebois, G., & Debenham, N. (2010). Une occupation de la phase ancienne du Paléolithique moyen à Therdonne (Oise). Chronostratigraphie, production de pointes Levallois et réduction des nucléus. *Gallia Préhistoire*, *52*, 1–32. https://doi.org/10.3406/galip.2010.2469
Mallegni, F. (1986). Les restes humains du gisement de Sedia del Diavolo (Rome) au Riss final. *L'Anthropologie*, *90*, 539–553.
Mania, D. (1991). The zonal division of the Lower Palaeolithic open-air site Bilzingsleben. *L'Anthropologie*, *XXIX*, 17–24.
Manzi, G., Salvadei, L., & Passarello, P. (1990). The Casal de' Pazzi archaic parietal: Comparative analysis of new fossil evidence from the late Middle Pleistocene of Rome. *Journal of Human Evolution*, *19*, 751–759. https://doi.org/10.1016/0047-2484(90)90019-8
Martínez-Pillado, V., Aranburu, A., Arsuaga, J., Ruiz-Zapata, B., Gil-García, M., Stoll, H., et al. (2014). Upper Pleistocene and Holocene palaeoenvironmental records in Cueva Mayor karst (Atapuerca, Spain) from different proxies: Speleothem crystal fabrics, palynology, and archaeology. *International Journal of Speleology*, *43*, 1–14. https://doi.org/10.5038/1827-806X.43.1.1
Martínez-Pillado, Virginia, Aranburu, A., Yusta, I., Stoll, H., & Arsuaga, J. L. (2010). Clima y ocupaciones en la Galería de Estatuas (Atapuerca, Burgos) en los últimos 14.000 años: Relatos de una estalagmita. *Munibe*, *61*, 89–102.
Mazza, P. P. A., Martini, F., Sala, B., Magi, M., Colombini, M. P., Giachi, G., et al. (2006). A new Palaeolithic discovery: Tar-hafted stone tools in a European Mid-Pleistocene bone-bearing bed. *Journal of Archaeological Science*, *33*, 1310–1318. https://doi.org/10.1016/j.jas.2006.01.006

Mercier, N., Froget, L., Miallier, D., Pilleyre, T., Sanzelle, S., & Tribolo, C. (2004). Nouvelles données chronologiques pour le site de Menez-Dregan 1 (Bretagne) : L'apport de la thermoluminescence. *Quaternaire*, *15*, 253–261. https://doi.org/10.3406/quate.2004.1772

Moigne, A.-M., Palombo, M. R., Belda, V., Heriech-Briki, D., Kacimi, S., Lacombat, F., et al. (2006). Les faunes de grands mammifères de la Caune de l'Arago (Tautavel) dans le cadre biochronologique des faunes du Pléistocène moyen italien. *L'Anthropologie*, *110*(5), 788–831. https://doi.org/10.1016/j.anthro.2006.10.011

Moncel, M. H. (2008). *Le site de Payre. Occupations humaines dans la vallée du Rhône à la fin du Pléistocène moyen et au début du Pléistocène supérieur*. Paris, France: Mémoire XLVI de la Société Préhistorique Française.

Monnier, Jean-Laurent, Hallégouet, B., Hinguant, S., Laurent, M., Auguste, P., Bahain, J.-J., et al. (1994). A new regional group of the Lower Palaeolithic in Brittany (France), recently dated by Electron Spin Résonance. *Compte rendus de l'Académie des Sciences de Paris*, *319*(II), 155–160.

Monnier, J.-L., Hallegouët, B., Hinguant, S., & Molines, N. (2001). La datation de l'habitat paléolithique inférieur de Menez-Dregan 1 (Plouhinec, Finistère, France). In J.-N. Barrandon, P. Guibert, & V. Michel (Eds.), *Argumentation géologique et archéologique: Datation. XXIes rencontres internationales d'archéologie et d'histoire d'Antibes, 19-21 octobre, 2000* (pp. 261–277). Éditions APDCA, Antibes.

Nagra, G., Treble, P. C., Andersen, M. S., Bajo, P., Hellstrom, J., & Baker, A. (2017). Dating stalagmites in mediterranean climates using annual trace element cycles. *Scientific Reports*, *7*, 621. https://doi.org/10.1038/s41598-017-00474-4

Neruda, P., & Nerudová, Z. (2009). *Moravský Krumlov IV - vícevrstvá lokalita ze středního a počátku mladého paleolitu na Moravě* (Vol. 29, N.S. 21, 2009). Brno: Moravské zemské muzeum.

Ollé, A., Vergès, J. M., Rodríguez-Álvarez, X. P., Cáceres, I., Angelucci, D. E., Vallverdú, J., et al. (2016). The Middle Pleistocene site of La Cansaladeta (Tarragona, Spain): Stratigraphic and archaeological succession. *Quaternary International*, *393*, 137–157. https://doi.org/10.1016/j.quaint.2015.08.053

Paul, B., Petrus, J., Savard, D., Woodhead, J., Hergt, J., Greig, A., et al. (2023). Time resolved trace element calibration strategies for LA-ICP-MS. *Journal of Analytical Atomic Spectrometry*, *38*, 1995–2006. https://doi.org/10.1039/D3JA00037K

Pereira, A. (2017b, October 17). *Apport de la datation 40Ar/39Ar à la compréhension de l'évolution culturelle des pré-néanderthaliens en Italie centrale et méridionale entre 750 et 250 ka* (PhD). Museum national d'histoire naturelle - MNHN PARIS, Università degli studi, Ferrare, Italie.

Perrette, Y., Delannoy, J. J., Desmet, M., Lignier, V., & Destombes, J. L. (2005). Speleothem organic matter content imaging. The use of a Fluorescence Index to characterise the maximum emission wavelength. *Chemical Geology*, *214*, 193–208. https://doi.org/10.1016/j.chemgeo.2004.09.002

Preece, R. C., Gowlett, J. A. J., Parfitt, S. A., Bridgland, D. R., & Lewis, S. G. (2006). Humans in the Hoxnian: Habitat, context and fire use at Beeches Pit, West Stow, Suffolk, UK. *Journal of Quaternary Science*, *21*, 485–496. https://doi.org/10.1002/jqs.1043

Ravon, A. L., García-Medrano, P., Moncel, M. H., & Ashton, N. (2022). Acheulean variability in Western Europe: The case of Menez-Dregan I (Plouhinec, Finistère, France). *Journal of Human Evolution*, *162*, 103103. https://doi.org/10.1016/j.jhevol.2021.103103

Rigaud, J. P., & Geneste, J. M. (1988). L'utilisation de l'espace dans la grotte Vaufrey. In *La grotte Vaufrey* (pp. 593–611). Mémoire de la Société Préhistorique Française.

Rigaud, J.-P. (1988). *La Grotte Vaufrey - Paléoenvironnement, chronologie, activités humaines*. Paris, France: Mémoire XIX de la Société Préhistorique Française.

Roebroeks, W. (1988). *From find scatters to early hominid behaviour: A study of Middle Palaeolithic riverside settlements at Maastricht-Belvédère (The Netherlands)*. University of Leiden: Analecta Praehistorica Leidensia 21.

Sañudo, P., Blasco, R., & Fernández Peris, J. (2016). Site formation dynamics and human occupations at Bolomor Cave (Valencia, Spain): An archaeostratigraphic analysis of levels I to XII (100–200 ka). *Quaternary International*, *417*, 94–104. https://doi.org/10.1016/j.quaint.2015.09.044

Sanz, M., Daura, J., Cabanes, D., Égüez, N., Carrancho, Á., Badal, E., et al. (2020). Early evidence of fire in south-western Europe: The Acheulean site of Gruta da Aroeira (Torres Novas, Portugal). *Scientific Reports*, *10*, 12053. https://doi.org/10.1038/s41598-020-68839-w

Sanz, M., Sala, N., Daura, J., Pantoja-Pérez, A., Santos, E., Zilhão, J., & Arsuaga, J. L. (2018). Taphonomic inferences about Middle Pleistocene hominins: The human cranium of Gruta da Aroeira (Portugal). *American Journal of Physical Anthropology*, *167*, 615–627. https://doi.org/10.1002/ajpa.23689

Savard, D., Dare, S., Bédard, L. P., & Barnes, S. J. (2023). A new mapping protocol for laser ablation (with fast-funnel) coupled to a time-of-flight mass spectrometer (LA-FF-ICP-ToF-MS) for the rapid, simultaneous quantification of multiple minerals. *Geostandards and Geoanalytical Research*, *47*, 243–265. https://doi.org/10.1111/ggr.12482

Schafer, D., & Jager, K. (1984). Verkohlte Steinkerne der Kornelkirsche (Cornus Mas L.) aus dem Paläolithikum des oberen Travertins von Weimar-Ehringsdorf. *Alt-Thuringen*, *20*, 15–22.

Schiegl, S., & Thieme, H. (2007). Auf den Spuren von Feuer in Schöningen 13 II-4. Ein Befund von Weltbedeutung: Ein Wildpferd-Jagdlager vor 400.000 Jahren. In H. Thieme (Ed.), *Die Schöninger Speere e Mensch und Jagd vor 400.000 Jahren* (pp. 166–171). Stuttgart.

Schmidt, E. D., Frechen, M., Murray, A. S., Tsukamoto, S., & Bittmann, F. (2011). Luminescence chronology of the loess record from the Tönchesberg section: A comparison of using quartz and feldspar as dosimeter to extend the age range beyond the Eemian. *Quaternary International*, *234*(1), 10–22. https://doi.org/10.1016/j.quaint.2010.07.012

Schvoerer, M., Rouanet, J.-F., Navaukkes, H., & Debénath, A. (1977). Datation absolue par thermoluminescence de restes humains antéwürmiens de l'Abri Suard a La Chaise-de-Vouthon (Charente). *Comptes rendus de l'Académie des science*, *284*(d), 1979–1982.

Shahack-Gross, R., Berna, F., Karkanas, P., Lemorini, C., Gopher, A., & Barkai, R. (2014). Evidence for the repeated use of a central hearth at Middle Pleistocene (300 ky ago) Qesem Cave, Israel. *Journal of Archaeological Science*, *44*, 12–21. https://doi.org/10.1016/j.jas.2013.11.015

Soriano, S., & Villa, P. (2017). Early Levallois and the beginning of the Middle Paleolithic in central Italy. *PLoS One*, *12*, e0186082. https://doi.org/10.1371/journal.pone.0186082

Soukup, V., & Mechurová, Z. (2018). Záhadný pravěký Samuel: Homo erectus paleohungaricus v kontextu antropogeneze [Mysterious prehistoric Samuel: *Homo erectus paleohungaricus* in the context of anthropogenesis]. *Anthropologia integra*, *9*(2), 7. https://doi.org/10.5817/AI2018-2-7

Stancampiano, L.M., Rubio-Jara, S., Panera, J., Uribelarrea, D., Pérez-González, A., & Magill, C.R. (2023). Organic geochemical evidence of human-controlled fires at Acheulean site of Valdocarros II (Spain, 245 kya). *Scientific Reports 13,* 7119. https://doi.org/10.1038/s41598-023-32673-7

Stapert, D. (2007). Youngsters knapping flint near the campfire: An alternative view of site k at Maastricht-Belvédère (the Netherlands). *Archaologisches Korrespondenzblatt*, *37*(1), 19–35.

Steiner, W. (1975). Zur stratigraphischen Stellung des Travertinprofils von Ehringsdorf bei Weimar [La position chronologique de la coupe dans les travertins d'Ehringsdorf près de Weimar]. *Alt-Thuringen*, *13*, 7–16.

Stepanchuk, V. N., & Moigne, A.-M. (2016). MIS 11-locality of Medzhibozh, Ukraine: Archaeological and paleozoological evidence. *Quaternary International*, *409*, 241–254. https://doi.org/10.1016/j.quaint.2015.09.050

Stratus, L. G. (1989). On early hominid use of fire. *Current Anthropology*, *30*, 488–491. https://doi.org/10.1086/203772

Street, M., Terberger, T., & Orschiedt, J. (2006). A critical review of the German Paleolithic hominin record. *Journal of Human Evolution*, *51*, 551–579. https://doi.org/10.1016/j.jhevol.2006.04.014

Suchý, V., Borecká, L., Pachnerová Brabcová, K., Havelcová, M., Svetlik, I., Machovič, V., et al. (2021). Microbial signatures from speleothems: A petrographic and scanning electron microscopy study of coralloids from the Koněprusy Caves (the Bohemian Karst, Czech Republic). *Sedimentology*, *68*, 1198–1226. https://doi.org/10.1111/sed.12826

Trinkaus, E., Marks, A. E., Brugal, J. P., Bailey, S. E., Rink, W. J., & Richter, D. (2003). Later Middle Pleistocene human remains from the Almonda Karstic system, Torres Novas, Portugal. *Journal of Human Evolution*, *45*, 219–226. https://doi.org/10.1016/j.jhevol.2003.07.001

Tuffreau, A., & Sommé, J. (1989). *Le gisement paléolithique moyen de Biache-Saint-Vaast (Pas de Calais). 1ère partie. Stratigraphie, environnement, études archéologiques* (Vol. 21). Paris, France: Mémoire Société Préhistorique Française.

Valladas, H., Mercier, N., Falguères, C., & Bahain, J.-J. (1999). Contribution des méthodes nucléaires à la chronologie des cultures paléolithiques entre 300 000 et 35 000 ans BP. *Gallia Préhistoire*, *41*(1), 153–166. https://doi.org/10.3406/galip.1999.2163

Valoch, K. (2003). Výzkum staropaleolitické lokality Stránská skála I v Brně-Slatině. *Acta Musei Moraviae*, *88*(1–2), 3–65.

Vandevelde, S., Brochier, J. É., Petit, C., & Slimak, L. (2017). Establishment of occupation chronicles in Grotte Mandrin using sooted concretions: Rethinking the Middle to Upper Paleolithic transition. *Journal of Human Evolution*, *112*, 70–78. https://doi.org/10.1016/j.jhevol.2017.07.016

Vandevelde, S., T. Boucherat, A. Bonneau, D. Deldicque, L. Marié, L. Slimak, & Petit, C. (2023). ExTraS program: Documenting the processes of fixation, recording, and preservation of combustion products in speleothems. *Archaeological and Anthropological Sciences, 15, 169*. https://doi.org/10.1007/s12520-023-01869-3.

Vertes, L., & Dobosi, V. T. (1990). Fireplaces of the settlement. In Miklós Kretzoi & V. T. Dobosi (Eds.), *Vértesszöllös site, man and culture* (pp. 519–521). Budapest: Akademiai Kiado.

Vieillevigne, E., Bourguignon, L., Ortega, I., & Guibert, P. (2008). Analyse croisée des données chronologiques et des industries lithiques dans le grand sud-ouest de la France (OIS 10 à 3). *PALEO. Revue d'archéologie préhistorique*, (20), 145–166. https://doi.org/10.4000/paleo.1715

Villa, P. (1983). *Terra Amata and the Middle Pleistocene archaeological record of southern France* (Vol. 13). University of California Press.

Villa, P. (1991). Middle Pleistocene prehistory in southwestern europe: The state of our knowledge and ignorance. *Journal of Anthropological Research*, *47*, 193–217. https://doi.org/10.1086/jar.47.2.3630325

Walker, M. J., Anesin, D., Angelucci, D. E., Avilés-Fernández, A., Berna, F., Buitrago-López, A. T., et al. (2016). Combustion at the late Early Pleistocene site of Cueva Negra del Estrecho del Río Quípar (Murcia, Spain). *Antiquity*, *90*, 571–589. https://doi.org/10.15184/aqy.2016.91

Zohar, I., Alperson-Afil, N., Goren-Inbar, N., Prévost, M., Tütken, T., Sisma-Ventura, G., et al. (2022). Evidence for the cooking of fish 780,000 years ago at Gesher Benot Ya'aqov, Israel. *Nature Ecology & Evolution*, *6*, 2016–2028. https://doi.org/10.1038/s41559-022-01910-z